



HAL
open science

Prebiotics Modify Host Metabolism in Rainbow Trout (Oncorhynchus Mykiss) Fed with a Total Plant-Based Diet: Potential Implications for Microbiome-Mediated Diet Optimization

Jep Lokesh, Mylène Ghislain, Marine Reyrolle, Mickael Le Béhec, Thierry Pigot, Frederic Terrier, Jérôme Roy, Stéphane Panserat, Karine Ricaud

► To cite this version:

Jep Lokesh, Mylène Ghislain, Marine Reyrolle, Mickael Le Béhec, Thierry Pigot, et al.. Prebiotics Modify Host Metabolism in Rainbow Trout (Oncorhynchus Mykiss) Fed with a Total Plant-Based Diet: Potential Implications for Microbiome-Mediated Diet Optimization. *Aquaculture*, 2022, 561, pp.738699. 10.1016/j.aquaculture.2022.738699 . hal-03763673

HAL Id: hal-03763673

<https://univ-pau.hal.science/hal-03763673v1>

Submitted on 29 Aug 2022

HAL is a multi-disciplinary open access archive for the deposit and dissemination of scientific research documents, whether they are published or not. The documents may come from teaching and research institutions in France or abroad, or from public or private research centers.

L'archive ouverte pluridisciplinaire **HAL**, est destinée au dépôt et à la diffusion de documents scientifiques de niveau recherche, publiés ou non, émanant des établissements d'enseignement et de recherche français ou étrangers, des laboratoires publics ou privés.

Prebiotics Modify Host Metabolism in Rainbow Trout (*Oncorhynchus Mykiss*) Fed with a Total Plant-Based Diet: Potential Implications for Microbiome-Mediated Diet Optimization

Jep Lokesh

University of Pau and Pays de l'Adour: Universite de Pau et des Pays de l'Adour

Mylène Ghislain

University of Pau and Pays de l'Adour: Universite de Pau et des Pays de l'Adour

Marine Reyrolle

University of Pau and Pays de l'Adour: Universite de Pau et des Pays de l'Adour

Mickael Le Behec

University of Pau and Pays de l'Adour: Universite de Pau et des Pays de l'Adour

Thierry Pigot

University of Pau and Pays de l'Adour: Universite de Pau et des Pays de l'Adour

Frédéric Terrier

University of Pau and the Adour Region: Universite de Pau et des Pays de l'Adour

Jérôme Roy

University of Pau and the Adour Region: Universite de Pau et des Pays de l'Adour

Stéphane Panserat

University of Pau and the Adour Region: Universite de Pau et des Pays de l'Adour

Karine Ricaud (✉ karine.brugirardricaud@univ-pau.fr)

Université de Pau et des Pays de l'Adour: Universite de Pau et des Pays de l'Adour

<https://orcid.org/0000-0003-3839-3121>

Research

Keywords: Rainbow trout, prebiotics, Mycoplasma, Firmicutes, Short chain fatty acid, aquaculture, microbiome, sustainable diet, metabolism

Posted Date: July 14th, 2021

DOI: <https://doi.org/10.21203/rs.3.rs-703272/v1>

License: © ⓘ This work is licensed under a Creative Commons Attribution 4.0 International License.

[Read Full License](#)

Abstract

Background

The use of plant-based ingredients in aquafeeds is increasing because marine sources of protein and oil are unsustainable. However, plant-based ingredients cause certain metabolic complications in carnivorous species such as rainbow trout. Here, we examined whether prebiotics have the potential to affect the metabolism of juvenile trout (Average weight: 25.88 ± 0.91 g) via microbially derived short-chain fatty acids (SCFAs). Fructo-oligosaccharides (FOS), inulin or mannan-oligosaccharides (MOS) were used at 1% or 2% in a 12-week feeding experiment. We measured changes in the intestinal microbiome, SCFA levels and metabolic responses in the intestine, liver, muscle, and adipose tissue.

Results

In the intestine, gene expression and SCFA production did not change significantly with prebiotics, although the MOS fed groups were clustered differently. Prebiotics had a significant effect on the abundance of *Bacillus*, *Lactobacillus* and *Weissella*, although posterior intestinal microbial diversity and composition did not change significantly after feeding prebiotics. Two operational taxonomic units (OTUs) belonging to *Mycoplasma* dominated all samples with an average relative abundance of >95% per group. Intestinal microvillar structures were significantly improved in length in the inulin-fed groups.

Systemically, overall hepatic gene expression was significantly different from control with inulin-fed groups showing upregulation of several metabolic and the fatty acid receptor genes. MOS fed groups showed a dose-dependent but contrasting response in liver and muscle. In addition, a significant reduction in final weight and SGR was observed in MOS fed at 1%. The relative abundance of OTUs belonging to *Lactobacillus* and *Bacillus* correlated with hepatic gene expression and final weight of the fish.

Conclusions

Inulin and MOS appear to differentially affect host metabolism, mainly in the liver and muscle. Differential abundance of *Lactobacillus* and *Bacillus* in the prebiotic-fed groups and their correlations with hepatic gene expression could indicate a prebiotic-microbiome-host axis, although this was not conclusively shown through the levels of SCFAs. In combination with a total plant-based diet, inulin could be a promising prebiotic for trout but need to be further investigated. These findings could implicate in microbiome-mediated dietary optimization of rainbow trout.

Background

Rainbow trout (*Oncorhynchus mykiss*) is an important carnivorous species in aquaculture, with a total worldwide production of 861,000 metric tonnes in 2018 [1]. Traditionally, aquaculture diets have relied heavily on the protein and oil from marine fish. However, this practice is environmentally unsustainable

as natural fish stocks are subject to severe fishing pressure. In addition, the constant shortage and rising cost of fishmeal and oil negatively affect the economic viability of the industry [2]. This necessitates a sustainable alternative diet devoid of fish meal and oil for the continued growth of the industry [2]. Significant research effort has been devoted to the development of alternative diets for rainbow trout by completely replacing marine protein and oil with vegetal protein and oil [3–7]. Although this approach has been successful in reducing the use of fish meal and oil in aquafeeds, culture-related traits, such as growth rate and gut health, have been negatively affected in some cases [8]. Furthermore, these alternative diets may also have an obesogenic effect on fish [9]. Therefore, it is necessary to improve and optimize the total plant-based diets in terms of use for growth and mitigation of adipogenic effects.

One of the strategies to improve the total plant-based diets would be the use of dietary supplements such as the prebiotics. Prebiotics are non-digestible mono- or polysaccharides used in diets of humans [10], livestock [11], and fish and shellfish [12–14]. Prebiotics are generally indigestible to the host and are specifically fermented by anaerobic bacteria in the distal intestine, resulting in various secondary metabolites, mainly short chain fatty acids (SCFAs) [10,15]. SCFAs such as butyrate, acetate and propionate are a significant source of energy for intestinal epithelial cells [16] and have local and systemic immunomodulatory effects [17]. In addition, these SCFAs are transported to various metabolic organs such as the liver [18], skeletal muscle [19], and adipose tissue [20,21] and exert their effects on various aspects of metabolism that are beneficial to the host. These SCFAs may be useful in overcoming some of the detrimental effects of total plant-based diets on carnivorous species such as rainbow trout.

Prebiotics have been used in aquatic animal diets for decades. Several studies have demonstrated the beneficial effects of prebiotics on the growth and health of various aquatic species [12,14]. The mechanisms of utilization of prebiotics and the role of the resulting metabolites (mainly SCFAs) in host metabolism are not well understood in aquatic organisms, especially in carnivorous species such as rainbow trout. Studies concerning the effects of prebiotics on trout are few and far between [22–26]. Most of these studies have been conducted in the context of growth and disease resistance [24–26] using fish meal and oil based basal diet.

The efficacy of a prebiotic in aquatic animals may vary depending on the species, feeding habits, composition of the intestinal microbiome, type of basal diet (fish meal or plant-based), and type of the prebiotic [13,14]. Knowledge of tissue-specific responses to these molecules is also limited. Thus, it is important to test different prebiotics by measuring both local effects (responses in the intestine) and systemic effects (responses in different metabolic organs).

Therefore, the objective of this study is to understand the effects (both in the intestine and in other metabolic organs) of different types of prebiotics in rainbow trout fed a 100 % plant-based basal diet. For this purpose, rainbow trout were fed with three different prebiotics, namely fructo-oligosaccharides (FOS), mannan-oligosaccharides (MOS) and inulin at two different doses ($1\text{g}^{-100\text{g}}$ and $2\text{g}^{-100\text{g}}$ feed) for 12 weeks and then intestinal microbiome, metabolites and structural changes were studied to understand the local effects of the prebiotics and their metabolites. Furthermore, the expression of metabolism- and

inflammation-related genes in the intestine was analysed. In order to assess the systemic responses, we analysed the expression of genes involved in different metabolic pathways and putative SCFA receptors in metabolic tissues such as liver, skeletal muscle and adipose tissue.

Results

Whole body composition, zootechnical, hepatic and plasma parameters

At the end of the feeding trial, whole-body protein, lipid, energy and ash contents did not differ significantly between groups ($p>0.05$; supplementary table 3). We measured different zootechnical parameters such as final weight, specific growth rate (SGR) and feed efficiency (FE). Plasma parameters such as glucose, triglycerides, free fatty acids, cholesterol and total amino acids were also measured. A one-way ANOVA revealed that the final weight was significantly affected by inclusion of prebiotics in the diet ($p<0.001$). Post-hoc comparison using Tukey's HSD revealed that body weight was significantly lower in the MOS1 group compared to the control (Table 2). Similarly, SGR was also affected by prebiotic feeding ($p<0.05$; Table 2). The highest mean SGR was observed in the inulin2 group (2.21) and the lowest in the MOS1 group (1.95). Post-hoc tests revealed no significant difference in the mean values compared to the control group (Table 2). FE and protein efficiency ratio were not significantly affected by the prebiotics ($p>0.05$; Table 2), although the mean values of all prebiotic groups were relatively higher than those of control group. The hepatosomatic index (HIS) was significantly affected by the prebiotic diet ($p<0.05$; Table 2), although group-specific differences were not detected compared to the control group. The viscerosomatic index (VSI) and all plasma parameters were not affected by the inclusion of the prebiotics in the diet ($p>0.05$; Table 2). None of the liver and plasma parameters measured in the current study were affected by dietary inclusions of the prebiotics ($p>0.05$; Table 3).

Microbial diversity and composition

Sequence data were rarefied to 24000 sequences per sample. Alpha diversity was calculated using the observed OTUs (Figure 1a) and the Shannon index (Figure 1b). Both measures were not significantly different between the control and prebiotic groups (ANOVA; $p>0.05$). Beta diversity was calculated using the Bray-Curtis dissimilarity index and visualised using NMDS ordination (Figure 1c). Homogeneity of group dispersions was checked using the PERMDISP ($p>0.05$). Groups were compared using a pairwise PERMANOVA, which showed no significant difference between feeding groups ($p>0.05$).

We identified 1790 OTUs belonging to 16 phyla. Among all OTUs, the top 20 most abundant OTUs occupied almost 100% of the reads in all feeding groups (Figure 2a). These 20 most abundant OTUs belonged to only 4 phyla, namely Fusobacteria, Firmicutes, Proteobacteria and Tenericutes. These included the genera *Aeromonas*, *Cetobacterium*, *Moraxella*, *Mycoplasma*, *Pseudomonas*, *Ralstonia*, *Streptococcus* and *Weissella* (Figure 2a). Two OTUs (OTU1 and OTU2) belonging to the genus *Mycoplasma* were the most abundant, with more than 96% of reads assigned to these OTUs in each group (Figure 2a). Between these two OTUs, OTU1 was significantly higher ($p<0.001$) in each group except inulin2 (Figure 2b).

***Firmicutes* in the intestine of rainbow trout**

Because OTUs belonging to *Mycoplasma* overshadowed the abundance of other OTUs, we additionally sequenced the V3-V4 region of the 16s rRNA of members of the phylum *Firmicutes* using a phylum-specific primer pair. The phylum *Firmicutes* and *Bacteroidetes* are known to harbour several species of polysaccharide-utilising bacteria in intestinal microbiome of animals [27]. Alpha ($p > 0.05$) and beta (PERMANOVA; $p > 0.05$) diversity did not differ significantly between dietary groups (Figure 2c). Although these primers were unable to avoid amplification of *Mycoplasma* and some members of the phylum *Proteobacteria*, we were able to detect several OTUs belonging to the phylum *Firmicutes*. More than 95% of the sequencing reads were assigned to the 20 most abundant OTUs (Figure 2d). These OTUs belong to the genera *Bacillus* (16.6%), *Gamella* (0.1%), *Lactobacillus* (10.5%), *Lactococcus* (0.2%), *Mycoplasma* (31.5%), *Staphylococcus* (0.7%), *Streptococcus* (5.6%) and *Weissella* (28.3%).

We performed supervised partial least square discriminant analysis (PLS-DA) to understand the dissimilarity of the diet groups in terms of their microbial composition. Only the OTUs, which were present at $> 0.1\%$ of the whole dataset, were retained for analysis. Although the clusters of the different dietary groups were not clearly separated by PLS-DA, the group means of ordination were clearly separated (Figure 3a). The regression coefficients of the discriminatory OTUs on component 1 of PLS-DA are shown (Figure 3b). Some of the most discriminatory OTUs belonged to *Bacillus*, *Lactobacillus* and *Weissella*. The correlation between these discriminatory OTUs and hepatic gene expression was evaluated using regularised canonical correlation analysis (rCCA). There was a positive correlation between the 3 OTUs belonging to the genus *Bacillus* (OTU3, OTU8 and OTU56) and genes involved in gluconeogenesis (*g6pcb1b*, *g6pca*, *pck1* and *fbp1b1*), glycolysis (*pfkla* and *pfklb*), energy metabolism (*sdhb*) and fatty acid beta-oxidation (*cpt1b* and *hoad*). On the other hand, two OTUs (OTU7 and OTU11) belonging to the genus *Lactobacillus* and one OTU each belonging to *Weissella* (OTU2) and *Alphaproteobacteria* (OTU5) were found to be negatively correlated with the above metabolic pathways (Figure 3c). Moreover, there was a significant effect of diet on the relative abundance of all these OTUs except OTU5 and the OTU2 ($p < 0.05$). Two OTUs belonging to the genus *Bacillus* (OTU8 and OTU56) were significantly higher ($p < 0.05$) in the MOS1 group than in the control (Figure 3d). In contrast, the relative abundance of OTU7 (*Lactobacillus*) was significantly lower in the MOS1 group (Figure 3d). It was also found that *Lactobacillus* (OTU11) and *Weissella* (OTU2) were positively correlated with final fish weight, while *Bacillus* (OTU3) and one OTU each belonging to *Streptococcus* and *Lactococcus* were negatively correlated with final weight (supplementary figure 1).

Short-chain fatty acids

The quantities of SCFAs did not differ significantly between the different groups ($p > 0.05$), although the MOS2 group had a higher quantity of all SCFA measured (Figure 4a). Clustering of the samples based on the count rates of the product ions derived from the SCFAs using PLS-DA showed different clustering of the two MOS groups and the inulin2 group (Figure 4b). Most of the discriminating features (product ions)

on component 1 of the PLS-DA belong to the MOS2, followed by MOS1 and inulin2. The product ions used for the detection of SCFAs are listed in supplementary table 4.

Intestinal morphology

In the current study, FOS and MOS groups did not show a drastic change in microvillar structure compared to the control. On the other hand, the two inulin groups showed significantly higher microvillar length compared to the control (Figure 5, supplementary figure 2). The attachment of the *Mycoplasma*-like organisms to the intestinal epithelial cell surface and the potential damage to the villous structure are shown in Figure 5h, Figure 5i, respectively.

Hepatic gene expression

We quantified the expression of several genes involved in amino acid metabolism, energy metabolism, fatty acid oxidation, fatty acid transformation, gluconeogenesis, glucose transport, glycolysis, lipogenesis and putative receptors for SCFAs in the liver.

ANOVA revealed that there was a significant effect ($p < 0.05$) of prebiotics on the expression of several genes involved in amino acid catabolism (*alat2*, *asat3*, *gdh2* and *gdh3*), energy metabolism (*atp5a*, *cox4*, *qcr2* and *sdhb*), fatty acid oxidation (*hoad*), fatty acid elongation (*fad*), gluconeogenesis (*fbp1b1*), glucose transport (*glut2a*, *glut2b*), glycolysis (*pfkla*, *pfklb*), and fatty acid receptors paralogues (*ffar31*, *ffar32*). Although these genes were generally expressed at higher level in the inulin groups (both 1% and 2%), no differences were detected between the control and the specific treatments using the Tukey's HSD, except for *sdhb*; significantly higher in inulin1 and MOS1, *fad*; significantly higher in inulin1 and MOS1, and *pfklb*; significantly higher in inulin2 and MOS2 (Figure 6a).

We also compared global hepatic gene expression using PERMANOVA between the control and the inulin and MOS groups. This showed significantly different clustering in the inulin1 group compared to the control ($p = 0.01$; Figure 6b). A similar comparison between the control and the MOS1 and MOS2 groups was not significant ($p > 0.05$), although the global expression pattern in the MOS1 group was similar to that of the control group, it was divergent from the MOS2 group ($p = 0.021$; Figure 6c).

Gene expression in muscle, intestine and adipose tissue

The expression of various genes in muscle was largely unaffected, with the exception of *gdh2* (amino acid catabolism), which was significantly lower in the inulin2 group ($p < 0.05$). Other genes affected by prebiotic feeding included *atp5a* and *qcr2* (energy metabolism) and *pfkmba*, which is involved in glycolysis (ANOVA; $p < 0.05$; Figure 7a). The global expression pattern in the MOS1 group was similar to the control, but significantly different from the MOS2 group (PERMANOVA; $p = 0.021$; Figure 7b).

In the intestine (supplementary figure 3a), the expression of *gdh1* (amino acid metabolism), *atp5a*, *cox2*, *cox4* (energy metabolism) was affected by the experimental diet as shown by ANOVA ($p < 0.05$), although the post-hoc test showed no group-wise difference ($p > 0.05$). In adipose tissue (supplementary figure 3b),

only the expression of *cox4*, *sdhb* (energy metabolism) and *cpt1b* (fatty acid oxidation) was affected by prebiotic feeding (ANOVA; $p < 0.05$). Tukey's HSD did not reveal any group-wise significant changes ($p > 0.05$).

Discussion

Prebiotics are widely used in aquaculture. Given the potential beneficial effects of prebiotics on growth, health and the intestinal microbiome [12,14], there is a need to demonstrate their mechanism of action in aquatic organisms, particularly in carnivorous species such as rainbow trout. In mammals, specific members of the phylum *Bacteroidetes*, *Firmicutes* and *Actinobacteria* have been shown to produce SCFAs by degrading the complex polysaccharides [27]. These SCFAs have been shown to affect host functions both in the intestine and systemically in liver, muscle and adipose tissue [15]. We adopted a similar approach in the current study, where we analysed the effect of different prebiotics both at the local level by examining the intestinal gene expression, gut morphology and metabolic output, and at the systemic level in terms of plasma metabolites and gene expressions in liver, muscle and adipose tissue.

The effect of prebiotics, possibly mediated via the intestinal microbiome on the intestinal health, has been noted in many teleost species [14]. In the present study, although there was an effect of prebiotics on a few genes in the energy metabolism pathway, there were no drastic changes in overall gene expression in the intestine. Diet-specific changes in SCFA content in the digesta were also not significant. Although, in the MOS2 group all the SCFAs seemed to be higher in general, it's hard to conclude about their functional importance due to high interindividual variation (specifically in the MOS2) and the small sample number ($n = 3$). On the other hand, the differences in abundance of OTUs belonging to *Bacillus* and *Lactobacillus* between dietary groups may be indicative of the microbial responses to prebiotics and interactions between microbial metabolites other than SCFAs and intestinal cells. Although species belonging to *Bacillus* and *Lactobacillus* are known to be widely used as probiotics in various teleosts [28], an in-depth analysis of their metabolic output at strain level and interaction with intestinal cells needs to be performed. Interestingly, the abundance of *Bacillus* and *Lactobacillus* was significantly altered only in the MOS1 group, which could be an indication of the type and dose specificity of the prebiotics, since these changes were not observed in the other types of prebiotics and the MOS fed at 2%. The dose-dependent differences in the effects of mannanoligosaccharides depending on dietary habits and life stages have been previously reported in teleosts [29]. The different host responses based on the variations in the molecular structures of different prebiotics and polysaccharide utilising enzyme repertoire (in the microbiome) are also plausible [30].

It has been shown that prebiotic feeding affects microvilli length and density in different teleosts [31,32]. We observed a significant effect of inulin on microvilli length. These structural changes are known to be mediated by the various microbial metabolites [33], although such relationships between microbial metabolites and intestinal morphology have not yet been demonstrated in teleosts. Damage to the tight junctions between cells has been observed in Arctic charr (*Salvelinus alpinus*) fed inulin at a dose of 15% [34] and in gilthead sea bream (*Sparus aurata*) [31]. Normally, this damage occurs due to inflammatory

responses [35], and such responses were not evident in the present study, as most inflammatory cytokines were either not expressed or the expression levels in the prebiotic groups were similar to the control.

In contrast to the intestine, at the systemic level, hepatic gene expression was significantly affected by inulin1 and a similar profile was observed in the inulin2 group. It is noteworthy that the effect of inulin was only observed in the liver, showing higher expression of several genes involved in the different metabolic pathways. It is interesting because these responses were observed with the concomitant higher expression of the potential fatty acid receptors (*ffar31* and *ffar32*), indicating a possible interaction between the liver and SCFA (or other similar microbial metabolites). Inulin has been implicated in glucose and lipid metabolism in rats [36] and mice [37], respectively. A recent study on tilapia showed that inulin resolved the metabolic syndrome induced by high carbohydrate [38]. The involvement of inulin in cholesterol metabolism by enhancing the activity of bile salt hydrolase (BSH), is well known. This enhancement leads to an increase in the biosynthesis of bile salts from cholesterol in the liver, resulting in a decrease in serum cholesterol levels [39]. In the current study, we did not observe any drastic change in serum cholesterol level.

On the other hand, it is interesting to note that these inulin-specific responses were not observed in intestine or muscle warranting further investigation of the metabolic output from inulin degradation and the mode of entry into the host, as well as the tissue specificity of the metabolites. Moreover, these hepatic gene expression changes observed in the inulin groups were not accompanied by the concomitant changes in the intestinal microbiome in the same group. Some previous studies have also noted the absence of changes in the intestinal bacterial composition in response to inulin in juvenile beluga (*Huso huso*) [40], red drum (*Sciaenops ocellatus*) [41] and hybrid striped bass (*Morone chrysops* × *Morone saxatilis*) [42]. This highlights the importance of application of meta-omic approaches to both host and the microbiome to understand the functional changes and molecular interactions that can occur without a drastic change in the composition.

Furthermore, the two MOS groups showed an opposite trend in gene expression with a significant difference in the overall expression profile between 1% and 2%. A similar contrast between MOS1 and MOS2 was also observed in muscle, but opposite to that of liver. The SCFA profile also clustered MOS1 and MOS2 separately. Overall, this may indicate a tissue-specific effect of these microbial metabolites between MOS1 and MOS2. The target metabolic organs of the microbial metabolites could vary [19]. In humans, the most abundant SCFA (butyrate) are generally thought to be utilized by colonocytes and the remaining SCFAs (propionate and acetate) are subject to hepatic metabolism. The class of metabolites affecting muscle metabolism could be complex, as both intestinal-derived metabolites and metabolites resulting from assimilation in the liver could interact with muscle [19]. While inulin had an effect on gene expression in the liver, absorption and transport of SCFA could not be confirmed in this study. The lack of differential expression of putative SCFA receptors (*ffar*) in the intestine could indicate a direct diffusion into cells or active uptake by previously unknown receptors. Apart from a few studies in zebrafish

showing interaction of microbial proteins with host beta cells [43] and neutrophils [44,45], receptor-mediated uptake of microbial proteins or metabolites has not been extensively demonstrated in teleosts.

To understand the role of the microbiome in utilisation of prebiotics, we analysed the intestinal bacterial composition. Interestingly, there was a high abundance (> 95%) of *Mycoplasma* in most of the samples. There are more than 100 species under the genus *Mycoplasma* associated with different organs in various animals and include both obligate symbionts and pathogens [46,47]. High abundance and prevalence of *Mycoplasma* has already been reported in salmonids [48–50]. A recent metagenome-derived characterization of intestinal *Mycoplasmas* from three salmonid species clearly indicates a strong coevolutionary mechanism between the host and *Mycoplasma* strains [51]. Moreover, the strains found in salmon and trout are quite closely related and clusters with a previously reported intracellular human respiratory and urogenital pathogen *Mycoplasma penetrans* [51]. Indeed, fluorescent *in situ* hybridization suggested that salmonid strains of *Mycoplasma* are intracellular [52]. The absence of pathogenicity genes in the salmonid strains [51] suggests a mutually beneficial relationship, as observed in the hadal sailfish, where the *Mycoplasma* is beneficial to the host by providing biotin in a nutrient-poor environment [53] and aiding in host defence [53,54]. In the present study, we observed 2 OTUs belonging to the genus *Mycoplasma* and they were differentially abundant in all feeding groups (except the inulin2 group). It needs to be confirmed whether these 2 OTUs actually belong to 2 different species of *Mycoplasma* and whether they have different potential to utilise different prebiotic molecules. Furthermore, we observed morphological structures resembling *Mycoplasma* on the microvilli of intestinal epithelial cells with a flask shape and a tip organelle, a typical feature of an intracellular *Mycoplasma* [55]. Similar structures were previously observed in another member of the salmonid family, Arctic charr [34]. The adhesion tendency of intracellular *Mycoplasma* to ciliated cells compared to secretory cells has been shown previously [55]. The damage to the ciliary structure and vacuolization inside the cells observed in the present study has been previously described in the case of infection of respiratory epithelial cells with *Mycoplasma pneumoniae* [56]. The consequences of such morphological changes on intestinal cell function and the fate of these *Mycoplasma* after entering the host cells need to be further investigated, either in an *in vitro* or *in vivo* setup.

Due to the overwhelming presence of *Mycoplasma* (> 99%) in most samples and the resulting extremely low read depth of other OTUs, we used *Firmicutes*-specific primers to investigate the abundance of OTUs under this phylum. This group is known to harbour several members involved in polysaccharide utilisation [27]. These primers were not able to fully discriminate OTUs belonging to *Mycoplasma* as they are known to be phylogenetically similar [46].

OTUs belonging to the *Bacillus* group were positively correlated with the expression of genes in glycolysis, gluconeogenesis, energy metabolism and fatty acid beta oxidation pathways. In contrast, OTUs belonging to the genus *Lactobacillus* and *Weissella* were negatively correlated with the expression of genes in the same metabolic pathways. The most striking correlation was with genes involved in gluconeogenesis. The association between glucose metabolism and microbiota has not been clearly established in teleosts. A recent study in zebrafish has shown the effect of a microbial (*Cetobacterium*

somerae) metabolite (acetate) on glucose homeostasis in zebrafish *via* the regulation of insulin secretion [57]. In addition, a microbial protein (*BefA*) has been shown to be involved in the differentiation of pancreatic B cells at early stages of zebrafish development [43]. In mammals, certain *Lactobacillus* species are known to inhibit gluconeogenesis by reducing the expression of phosphoenolpyruvate carboxykinase [58]. This effect is thought to be caused by different SCFAs (butyrate and propionate) *via* activation of the hepatic AMPK pathway [59]. On the other hand, the positive correlation between *Lactobacillus* and final weight could be due to the higher visceral fat, as there was also a positive correlation between *Lactobacillus* and visceral fat index. This could be an indication of the reduced entry of lipolysis related metabolites such as free fatty acid and glycerol into the gluconeogenic pathway [60]. *Bacillus* and its positive correlation with the gluconeogenic pathway and negative correlation with final fish weight is intriguing and needs further investigation. It should be mentioned that several members of *Lactobacillus* and *Bacillus* are used as probiotics in teleost aquaculture [28], with a wide range of beneficial effects on the host. Therefore, it is important to understand the genomes of OTUs belonging to *Bacillus* and *Lactobacillus* in the current study to describe the basis of the observed correlations with host metabolism. The significantly lower abundance of *Lactobacillus* and concomitant higher abundance of *Bacillus* in MOS1, and their opposite correlation with the expression of genes in hepatic metabolism collectively suggest a mechanism involving these two members of the *Firmicutes* and possibly their metabolites that alters hepatic metabolism and ultimately the fish growth in MOS1.

Conclusion

The present study showed that the polysaccharide inulin and mannan-oligosaccharides may have an effect on the expression of genes involved in various metabolic pathways in the metabolic organs, liver and muscle. The local effect of inulin in the intestine was limited in terms of gene expression, microbial composition and SCFAs, although the effect on microvillar structure was evident. On the other hand, MOS showed a dose-dependent difference in the abundance of bacterial groups (*Lactobacillus* and *Bacillus*).

Systemically, the effect of inulin and MOS was seen in the liver, whereas in muscle the response was dose-dependently restricted to MOS. The high abundance of *Mycoplasma* sp. in the trout intestine is an indication that it is an obligate symbiont of trout, and this host-*Mycoplasma* association requires further investigation to understand its role in trout physiology. The differential abundance of *Lactobacillus* and *Bacillus*, their correlations with metabolic gene expression and final weight, taken together, could be indicative of the prebiotic-microbiome-host axis. Nevertheless, studies on the recognition and uptake mechanisms of SCFAs in the intestine and their transport and assimilation in different metabolic organs need further investigation. The application of meta-omic approaches in future studies could provide insights into such interactions and open new opportunities for microbiome-mediated nutritional optimization in aquaculture.

Methods

Diet and experimental setup

A total plant-based diet either with (experimental) or without (control) different prebiotics was prepared. The formulation and proximate composition of the diet is given in table 1 and supplementary table 1, respectively. The diets were prepared to meet the nutritional requirements of the rainbow trout [61] and manufactured and tested at the INRAE experimental fish farm in Landes, France. The diets were isoproteic (~50% crude protein), isolipidic (~20% crude fat) and isoenergetic (~24 KJ^g dry matter). The experimental diet was supplemented with either fructo-oligosaccharides (FOS), inulin or mannan-oligosaccharides (MOS), each at 2 different doses, 1g^{-100g} and 2g^{-100g} feed. These doses were selected based on previous studies on various carnivorous teleosts [13]. The basal diet contained only the mixture of plant ingredients and vegetable oils supplemented by free amino acids. Thirty-six juvenile rainbow trout (~0.13g⁻¹) in equal numbers of males and females were randomly distributed in each of the 130 L fiberglass tanks. There were seven diet groups in total and 3 tanks were assigned to each of the diet groups. The fish were kept throughout the experimental period under standard rearing conditions with water oxygen levels 9 mg^{-L}, temperature 17 °C and pH 7.5, water flow rate 0.3L^{-s}, with daylight of 12h and 12h of darkness. The fish were manually fed twice a day (with an interval of 8h) either with the control diet or one of the experimental diets for 12 weeks. The tanks were checked for mortalities (if any) daily. The fish were weighed in bulk every three weeks to evaluate the growth parameters.

Sampling

After the feeding experiment, fish were randomly sampled from each tank 24 h after the last feeding. The randomly selected fish were first anaesthetised with benzocaine (30 mg-L) before being euthanized with a benzocaine overdose of 100 mg-L, followed by blood collection for plasma isolation. After the blood collection, fish were aseptically dissected and the digestive tract was separated. Liver, adipose and muscle were dissected and immediately frozen with liquid nitrogen and stored at -80 °C for long-term storage. The posterior intestine was separated from the rest of the digestive tract and was cut open longitudinally using sterile instruments. The posterior intestine was chosen because most polysaccharide-utilizing bacteria are found in the distal intestine of other animals. The contents and mucus were sampled together to analyse the total microbial profile of the intestine and a part of the tissue was also collected for the RNA extraction. Intestinal contents and distal intestinal tissue samples for SCFA and electron microscopy, respectively, were also flash frozen using liquid nitrogen and then stored at -80 °C.

Diet and whole-body proximate composition

Proximate composition was performed by the following methods. Dry matter was determined by drying the samples at 105 °C for 24 h. The weight of the post-dried samples was subtracted from the pre-dried samples. Ash content in the samples was measured by incinerating the samples at 550 °C for 16 h and comparing the weight of post-incinerated samples with the weight of the pre-incinerated samples. Protein content and lipid content were measured by the Kjeldahl and Kjeltex™ methods, respectively. The gross energy of the samples was measured using an adiabatic bomb calorimeter (IKA, Heitersheim Gribheimer, Germany).

Measurement of the plasma biochemical parameters

Blood samples were collected using the heparinised syringe and tubes. Samples were centrifuged at 3000 g for 10 min to isolate plasma and stored at -20°C until use. Commercial kits designed to be used along with the microplate reader were used to measure the plasma glucose (Glucose RTU, bioMérieux, Marcy l'Etoile, France), triglycerides (PAP 150, bioMérieux), cholesterol (Cholesterol RTU, bioMérieux) and free fatty acid (NEFA C kit, Wako Chemicals, Neuss, Germany). Total free amino acid was quantified according to the method of Moore [62], with glycine as standard.

Hepatic fat measurement

Hepatic fat was measured according to the protocol described previously [63]. The lyophilised liver samples (100mg) were mixed and homogenised with Folch reagent to extract the lipids. The lipids were extracted three times using this protocol and sodium chloride was added to the recovered supernatant after centrifugation for phase separation. The bottom layer containing the lipids was harvested and transferred to a glass tube, and the solvents were evaporated using nitrogen gas at 40°C. After drying, the lipids were weighed.

Hepatic glycogen measurement

Liver glycogen was measured according to the protocol described by Good et al [64]. Briefly, lyophilised liver (100 mg) was homogenised with 1M HCL (VWR, France). After this step, the samples were divided into 2 aliquots and one part was neutralised with 5M KOH (VWR), centrifuged and the supernatant was used to measure free glucose with a commercial kit (Glucose RTU, bioMérieux). The second aliquot was boiled with 5M KOH (VWR) for 2.5h at 100°C before neutralization. After centrifugation, total glucose (free glucose + glucose released by hydrolysis of glycogen) was measured in the supernatant. The glycogen content was calculated by subtracting the free glucose from the total glucose.

Microbiome analysis

DNA extraction

DNA from the mixture of intestinal contents and mucus was extracted using the QIAamp fast DNA stool kit (Qiagen, France) according to the manufacturer's instructions with the following modifications. Samples were mixed with Inhibitex buffer (1:7 ratio) and homogenized using zirconia beads (1.4 mm) in a 2-mL tube with a tissue homogenizer, Precellys[®]24 (Bertin technologies, Montigny le Bretonneux, France) at 5000 rpm for 30 sec. After homogenization, samples were incubated at 70 °C for 10 min instead of 1 min. These two modifications were performed for efficient lysis of cells that are difficult to lyse. DNA was checked for purity and integrity, and then quantified using NanoDrop 2000c (Thermo, Vantaa, Finland).

Generation of the 16s rRNA sequencing libraries

Libraries were prepared according to the standard protocol recommended by Illumina® [65]. The gene-specific region of the primer targeted the V3 and V4 regions of the 16s rRNA gene [66]. The illumina adapter overhang sequence was appended to the gene-specific region. The preparation of the amplicon sequencing library involved 2 stages of PCR. The first stage of PCR was a 25 µL reaction mixture consisting of 12.5 µL KAPA HiFi Mastermix (Roche, France), 5 µL (1µM) each of the forward (5'-TCGTCGGCAGCGTCAGATGTGTATAAGAGAC

AGCCTACGGGNGGCWGCAG-3') and reverse (5'-GTCTCGTGGGCTCGGAGATGT

GTATAAGAGACAGGACTACHVGGGTATCTAATCC-3') primers and 2.5 µL of DNA (~100 ng). Reactions were performed in duplicate for each sample. Thermocycling conditions included a pre-incubation for 3 min at 95 °C, followed by 35 cycles of denaturation at 95 °C for 30 sec, annealing at 55 °C for 30 sec, and extension at 72 °C for 30 sec. A final extension was performed at 72 °C for 5 min. The resulting PCR products were pooled for each sample and run on a gel to confirm amplification of a ~550 bp product. A positive and a negative control sample were also included in the run. After confirmation of PCR amplification, the PCR products were shipped to La Plateforme Génome Transcriptome de Bordeaux (PGTB, Bordeaux, France) for the following steps. Index PCR was performed to add the unique dual indexes to the sequences in a sample-specific manner. For this purpose, the Nextera XT index kit was used according to the manufacturer's protocol (Illumina, France). Thermocycling conditions were the same as in step 1, except that PCR was performed for only 8 cycles. After PCR clean-up, libraries were quantified using the KAPA library quantification kit for Illumina platforms (Roche, France) according to the manufacturer's instructions. Libraries were pooled at an equimolar concentration (4nM) and sequenced on a MiSeq platform using a 250 bp Paired End Sequencing Kit v2 (Illumina, France).

PCR conditions and sequencing protocol were also the same for *Firmicutes* amplicons using forward (5'TCGTCGGCAGCGTCAGATGTGTATAAGAGACAGGGCAGCAGTRGGGAATCTTC3') and reverse (5'GTCTCGTGGGCTCGGAGATGTGTATAAGAGACAGACACYTAGYACTCATCGTTT3') primers.

Data analysis

The initial data analysis was performed using the UPARSE pipeline [67]. First, the forward and reverse reads of each sample were fused. Also, the primer binding sites were removed from the assembled sequences. Then, the sequences were quality filtered using the strategy of filtering by the maximum expected error rate [68]. Sequences with an error rate of > 0.01 per sequence were removed from the dataset. After quality filtering, sequences from different samples were labelled with the sample name and combined in to a single file. This collection of sequences was dereplicated and the sequences that were observed only once in the dataset (singletons) were removed, as these singletons were most likely sequencing artefacts [69]. The sequences were further clustered into OTU (Operational Taxonomic Unit) based on a sequence similarity of 97%. The raw reads were then mapped back to the OTUs to obtain the abundance of each OTU in different samples. The taxonomy was assigned to the OTUs using SINTAX [70]. Taxonomies with bootstrap confidence value less than 0.8 were removed from the dataset.

Furthermore, OTUs belonging to the phylum *Chloroflexi* were removed from the analysis as it is likely that these OTUs originated from the plant components of the diet. A phylogenetic tree in Newick format was constructed based on the OTU sequences. The OTU table, taxonomy table and phylogenetic tree were imported into the phyloseq package [71] in R (version 3.6.3) along with the sample metadata. Alpha diversity measures, observed OTUs and Shannon index [72] were calculated. Beta diversity was calculated using the Bray-Curtis distance with the phyloseq package. All of these data analysis steps were also applied to the *Firmicutes* amplicon dataset.

Short-chain fatty acid measurement

Sample preparation

Frozen samples of intestinal contents were weighed and placed in 1-L glass bottles (Duran, Mainz, Germany) filled with clean air zero supplied by an F-DGS air zero generator (Evry, France). Screw caps with three GL14 ports (Duran) were used to connect the bottles directly to the heated inlet line (100 °C) of the SIFT-MS instrument via the sample inlet. A Tedlar bag (Zefon International Inc., Florida, USA), filled with dry and clean zero air and connected to the bottle inlet was used to compensate for the depression in the bottle during SIFT-MS sampling at a flow rate of 20 mL min⁻¹ [73,74]. The closed bottle was incubated at 60 °C ± 2 for 2 hours before SIFT-MS analysis.

Selected Ion Flow Tube – Mass Spectrometry (SIFT-MS) measurements

A Voice 200 Ultra SIFT-MS (SYFT Technologies, Christchurch, New Zealand) equipped with a dual source generating positive soft ionizing reagent ions (H₃O⁺, O₂^{●+}, NO⁺) with the nitrogen carrier gas (Air Liquid, Alphagaz 2) was used in this study.

Full-scan mass spectra were recorded for each positive precursor ion (H₃O⁺, O₂^{●+}, NO⁺) in a *m/z* range from 15 to 250 with an integration time of 60 s. Quantification was performed using the NO⁺ precursor ion. In SIFT-MS analysis, quantification is straightforward and requires only measurement of the count rate of the precursor ion [R] and product ions [P]. The analyte concentration in the flow tube [A] can be determined according to the following calculation:

$$[A] = \frac{[P]}{t_r k [R]}$$

where *t_r* is the reaction time in the flow tube and *k* is the apparent reaction rate constant.

Electron microscopy

Electron microscopic studies were performed at the Bordeaux Imaging Center - Bordeaux University, a Core facility of the French network “France Bio Imaging”. Intestinal samples were fixed with 2.5% (v/v) glutaraldehyde in 0.1M phosphate buffer (pH 7.4) for at least 2h at room temperature (RT) and stored at 4 °C until further processing. Samples were washed in 0.1M phosphate buffer and post-fixed in 1% (v/v)

osmium tetroxide in 0.1M phosphate buffer for 2h in the dark (RT), followed by washing in water. Dehydration (by a series of graded ethanol) and embedding preparations in epoxy resin (Epon 812; Delta Microscopy, Toulouse, France) were performed automatically using the automatic microwave tissue processor for electron microscopy (Leica EM AMW; Leica Microsystems, Vienna, Austria). Polymerization of the resin was carried out at 60 °C for a period of 24-48 hours. Samples were then sectioned using a diamond knife (Diatome, Biel-Bienne, Switzerland) on an ultramicrotome (EM UCT, Leica Microsystems, Vienna, Austria). Thick sections (500 nm) were prepared with toluidin blue staining to localize the region of interest. Then, ultrathin sections (70 nm) were picked up on copper grids and subsequently stained with uranyl acetate and lead citrate. The grids were examined with a transmission electron microscope (H7650, Hitachi, Tokyo, Japan) at 80kV.

Gene expression analysis

RNA from liver, intestine and muscle was extracted using TRIzol reagent method (Invitrogen, Carlsbad, CA) according to the manufacturer's protocol. RNA from adipose tissue was extracted using the RNeasy kit for fatty tissues (Qiagen, France). One µg RNA was converted to cDNA using the enzyme superscript III reverse transcriptase and random hexamers (Invitrogen, France) in the case of liver and muscle, while the quantinova reverse transcription kit (Qiagen, France) was used for adipose tissue and intestine. After the reverse transcription, cDNA was diluted 75-fold (liver) and 20-fold for muscle, adipose tissue and intestine before its use in RT-qPCR.

RT-qPCR was performed on a LightCycler[®] 384 system (Roche Diagnostics, Neuilly-sur-Seine, France). Reactions were performed on a 384 well plate. The total volume of reaction was 6 µL, consisting of 3 µL of LightCycler[®] SYBR Green I Master mix (Roche, France), 0.24 µL each of the forward and reverse primers at 200 nM, and 2 µL of cDNA diluted in DNase/RNase-free water (5 Prime GmbH, Hamburg, Germany). Thermocycling conditions included a pre-incubation at 95 °C for 10 min, followed by 45 cycles of denaturation at 98 °C for 15 sec, annealing at 60 °C for 10 sec and extension at 72 °C for 15 sec. Fluorescence data were recorded after each cycle at 72 °C. A melt curve analysis was performed to check the specificity of the primers. The C_q values were further converted to relative quantities considering the efficiency of each primer pair used in the study. The list of genes and details of the primers are shown in supplementary table 2. Relative quantities of each gene were then normalized against the normalization factors calculated for each tissue based on the geometric mean of the relative quantities of the 2 most stable reference genes across samples. These calculations were performed using geNorm [75], which is implemented in the R [76] package SLqPCR [77]. The reference genes *eef1a* and *rna18s* were used to calculate the normalization factor in liver, while a combination of *actb* and *eef1a* was used in muscle, *actb* and *eef1a* in adipose tissue, and *actb* and *rna18s* in intestine. Normalized relative quantities were analysed for statistical significance.

Statistical analysis

Zootechnical parameters, including feed efficiency (FE) and specific growth rate (SGR), are calculated per tank (n=3). HSI, VSI and final growth data are collected for each sampled individual (n=9). Samples from the same nine fish were also used for gene expression analysis and plasma parameters. For microbiome analysis, three fish were sampled in addition to the 9 already mentioned. Three additional fish per group were sampled for SCFA analysis and for electron microscopy.

All statistical analysis was performed using R software (version 3.6.3) [76]. Data were tested for normality of distribution and homogeneity of variance using the Shapiro-Wilk test and Bartlett's test, respectively. If these two assumptions were met, the data were analysed using one-way ANOVA followed by Tukey's HSD as a post hoc test. If the data were not normally distributed, Levene's test for homogeneity of variance was used. When variables did not follow either of the assumptions of normal distribution or equal variance, a non-parametric Kruskal-Wallis test followed by a pairwise Wilcoxon test was used.

Multivariate homogeneity of group dispersions (variances), as proposed in PERMDISP2 [78], was analysed using the '*betadisper*' function in the vegan package [79]. The statistical significance of Bray-Curtis distances between dietary groups was analysed using permutational multivariate analysis of variance: PERMANOVA [80], as implemented in the '*pairwise_adonis*' function of the ranacapa package [81]. *Firmicutes* data were analysed following the same steps. In addition, differences in community composition were analysed and visualised using supervised partial least square discriminant analysis (PLS-DA) as implemented in the mixOmics package [82]. The rCCA (regularised canonical correlation analysis) function of the same package was used to calculate the correlations between OTUs and hepatic gene expression, zootechnical and plasma parameters. Zero inflated OTU data were transformed using centered log transformation (clr).

Abbreviations

ANOVA

Analysis of variance

clr

Centered log transformation

FE

Feed efficiency

FOS

Fructo-oligosaccharides

HSI

Hepatosomatic index

MOS

Mannan-oligosaccharides

NMDS

Non-metric multidimensional scaling

OTU
Operational taxonomic unit
PERMANOVA
Permutational multivariate ANOVA
PERMDISP
Permutational analysis of multivariate dispersions
rCCA
Regularized canonical correlation analysis
SCFA
Short-chain fatty acid
SGR
Specific growth rate
PLS-DA
Partial least squares discriminant analysis
VSI
Viscerosomatic index

Declarations

Ethical approval

The experiment was conducted in accordance with the guidelines laid down by French and European legislation for the use and care of laboratory animals (Decree no. 2013–118, February 1st 2013 and Directive 2010/63/EU, respectively). The fish handling protocols and the sampling for this experiment were approved by the INRAE ethics committee (INRAE 2002-36, April 14, 2002). The INRAE experimental station (INRAE facilities of Donzacq, Landes, France) is certified for animal services under the licence number A40-228.1 by the French veterinary service, which is a competent authority.

Consent for publication

Not applicable

Availability of data and material

All sequence data are available at the NCBI sequence read archive under accession numbers PRJNA738672 and PRJNA738678.

Competing interests

The authors declare no conflict of interest.

Funding

The current study was supported by the European Maritime and Fisheries Fund (FEAMP) AntiOB Grant to KR (22001230-00002811).

Author's contributions

JL designed and performed the wet lab experiments and data analysis, and drafted the first version of the paper. KR and SP conceived and coordinated the study. MG, MR, MLB and TP performed the SCFA analysis. FT formulated the diets and overlooked the experiment. JR designed the primers for the fatty acid receptors. All authors contributed to the review of the manuscript. All authors read and approved the final manuscript.

Acknowledgements

Imaging was performed at Bordeaux Imaging Center, member of the France Bioimaging national infrastructure (ANR-10-INBS-04). We thank Sabrina Lacomme for her TEM work on this project. We thank Franck Sandres and Anthony Lanuque, Fish experimental facility, Donzacq for feed preparation, experimental setup, monitoring of the experiment and sampling. We thank Charlotte Andrieux, Sandra Biasutti, Anne Surget and Michael Marchand for their help in sampling.

References

1. Food and agriculture organization of the united nations [FAO]. The state of world fisheries and aquaculture 2020 [Internet]. FAO; 2020 Jun. <http://www.fao.org/3/ca9229en/ca9229en.pdf>
2. Hua K, Cobcroft JM, Cole A, Condon K, Jerry DR, Mangott A, et al. The future of aquatic protein: Implications for protein sources in aquaculture diets. *One Earth*. 2019;1:316–29. <https://www.sciencedirect.com/science/article/pii/S2590332219301320>
3. Le Boucher R, Quillet E, Vandeputte M, Lecalvez JM, Goardon L, Chatain B, et al. Plant-based diet in rainbow trout (*Oncorhynchus mykiss*): Are there genotype-diet interactions for main production traits when fish are fed marine vs. plant-based diets from the first meal?. *Aquaculture*. 2011;321:41–8. <https://www.sciencedirect.com/science/article/pii/S004484861100634X?via%3Dihub>
4. Callet T, Médale F, Larroquet L, Surget A, Aguirre P, Kerneis T, et al. Successful selection of rainbow trout (*Oncorhynchus mykiss*) on their ability to grow with a diet completely devoid of fishmeal and fish oil, and correlated changes in nutritional traits. *PLoS One*. 2017;12:e0186705. <https://dx.plos.org/10.1371/journal.pone.0186705>
5. Geurden I, Borchert P, Balasubramanian MN, Schrama JW, Dupont-Nivet M, Quillet E, et al. The positive impact of the early-feeding of a plant-based diet on its future acceptance and utilisation in rainbow trout. *PLoS One*. 2013;8:e83162. <https://dx.plos.org/10.1371/journal.pone.0083162>
6. Cottrell RS, Blanchard JL, Halpern BS, Metian M, Froehlich HE. Global adoption of novel aquaculture feeds could substantially reduce forage fish demand by 2030. *Nat Food*. 2020;1:301–8. <https://www.nature.com/articles/s43016-020-0078-x>

7. Napier JA, Haslam RP, Olsen RE, Tocher DR, Betancor MB. Agriculture can help aquaculture become greener [Internet]. *Nat. Food*. Springer Nature; 2020. p. 680–3.
<https://www.nature.com/articles/s43016-020-00182-9>
8. Glencross BD. A feed is still only as good as its ingredients: An update on the nutritional research strategies for the optimal evaluation of ingredients for aquaculture feeds. *Aquac Nutr*. 2020;26:1871–83. <https://onlinelibrary.wiley.com/doi/full/10.1111/anu.13138>
9. Panserat S, Hortopan GA, Plagnes-Juan E, Kolditz C, Lansard M, Skiba-Cassy S, et al. Differential gene expression after total replacement of dietary fish meal and fish oil by plant products in rainbow trout (*Oncorhynchus mykiss*) liver. *Aquaculture*. 2009;294:123–31.
<https://www.sciencedirect.com/science/article/pii/S0044848609004992>
10. Bruzzese E, Volpicelli M, Squaglia M, Tartaglione A, Guarino A. Impact of prebiotics on human health. *Dig Liver Dis*. 2006;38:S283–7.
<https://www.sciencedirect.com/science/article/pii/S1590865807600115>
11. Gaggia F, Mattarelli P, Biavati B. Probiotics and prebiotics in animal feeding for safe food production. *Int J Food Microbiol*. 2010;141:S15–28.
<https://www.sciencedirect.com/science/article/pii/S0168160510001121?via%3Dihub>
12. Song SK, Beck BR, Kim D, Park J, Kim J, Kim HD, et al. Prebiotics as immunostimulants in aquaculture: A review. *Fish Shellfish Immunol*. 2014;40:40–8.
<https://www.sciencedirect.com/science/article/pii/S1050464814002150>
13. Guerreiro I, Oliva-Teles A, Enes P. Prebiotics as functional ingredients: Focus on Mediterranean fish aquaculture. *Rev Aquac*. 2018;10:800–32.
<https://onlinelibrary.wiley.com/doi/abs/10.1111/raq.12201>
14. Ringø E, Olsen RE, Gifstad T, Dalmo RA, Amlund H, Hemre GI, et al. Prebiotics in aquaculture: A review. *Aquac Nutr*. 2010;16:117–36. <https://onlinelibrary.wiley.com/doi/10.1111/j.1365-2095.2009.00731.x>
15. Guarino MPL, Altomare A, Emerenziani S, Di Rosa C, Ribolsi M, Balestrieri P, et al. Mechanisms of action of prebiotics and their effects on gastro-intestinal disorders in adults. *Nutrients*. 2020;12.
<https://www.ncbi.nlm.nih.gov/pmc/articles/PMC7231265/>
16. Donohoe DR, Garge N, Zhang X, Sun W, O'Connell TM, Bunger MK, et al. The microbiome and butyrate regulate energy metabolism and autophagy in the mammalian colon. *Cell Metab*. 2011;13:517–26. <https://www.sciencedirect.com/science/article/pii/S1550413111001434?via%3Dihub>
17. Corrêa-Oliveira R, Fachi JL, Vieira A, Sato FT, Vinolo MAR. Regulation of immune cell function by short-chain fatty acids. *Clin Transl Immunol*. 2016;5:e73.
<https://www.ncbi.nlm.nih.gov/pmc/articles/PMC4855267/>
18. Shimizu H, Masujima Y, Ushiroda C, Mizushima R, Taira S, Ohue-Kitano R, et al. Dietary short-chain fatty acid intake improves the hepatic metabolic condition via FFAR3. *Sci Rep*. 2019;9:1–10.
<https://doi.org/10.1038/s41598-019-53242-x>

19. Frampton J, Murphy KG, Frost G, Chambers ES. Short-chain fatty acids as potential regulators of skeletal muscle metabolism and function. *Nat Metab.* 2020;2:840–8.
<https://www.nature.com/articles/s42255-020-0188-7>
20. Canfora EE, Jocken JW, Blaak EE. Short-chain fatty acids in control of body weight and insulin sensitivity. *Nat Rev Endocrinol.* 2015;11:577–91. <https://www.nature.com/articles/nrendo.2015.128>
21. Jocken JWE, Hernández MAG, Hoebbers NTH, van der Beek CM, Essers YPG, Blaak EE, et al. Short-chain fatty acids differentially affect intracellular lipolysis in a human white adipocyte model. *Front Endocrinol (Lausanne).* 2018;8:11. www.frontiersin.org
22. Yilmaz E, Genç M, Genç E. Effects of dietary mannan oligosaccharides on growth, body composition, and intestine and liver histology of rainbow trout, *Oncorhynchus mykiss*. *Isr J Aquac.* 2007;59:182–8. <https://avesis.erciyes.edu.tr/yayin/22680de5-8b5c-4f14-a468-3121a46db3fd/effects-of-dietary-mannan-oligosaccharides-on-growth-body-composition-and-intestine-and-liver-histology-of-rainbow-trout-oncorhynchus-mykiss>
23. Dimitroglou, A. The effect of dietary mannan oligosaccharides on the intestinal histology of rainbow trout (*Oncorhynchus mykiss*). *Comp Biochem Physiol Mol Integ Phys, A.* 2008;150:S63.
<https://ci.nii.ac.jp/naid/10029845460>
24. Staykov Y, Spring P, Denev S, Sweetman J. Effect of a mannan oligosaccharide on the growth performance and immune status of rainbow trout (*Oncorhynchus mykiss*). *Aquac Int.* 2007;15:153–61. <https://link.springer.com/article/10.1007/s10499-007-9096-z>
25. Rodriguez -Estrada U, Satoh S, Haga Y, Fushimi H, Sweetman J. Effects of single and combined supplementation of *Enterococcus faecalis*, mannan oligosaccharide and polyhydroxybutyrate acid on growth performance and immune response of rainbow trout *Oncorhynchus mykiss*. *Aquac Sci.* 2009;57:609–17. <https://www.semanticscholar.org/paper/Effects-of-single-and-combined-supplementation-of-Estrada-Satoh/901423e2afd8719b2390a7007a3b1795598c2f46>
26. Rodriguez-Estrada U, Satoh S, Haga Y, Fushimi H, Sweetman J. Effects of inactivated *Enterococcus faecalis* and mannan oligosaccharide and their combination on growth, immunity, and disease protection in rainbow trout. *N Am J Aquac.* 2013;75:416–28.
<https://www.tandfonline.com/doi/abs/10.1080/15222055.2013.799620>
27. Kaoutari A El, Armougom F, Gordon JI, Raoult D, Henrissat B. The abundance and variety of carbohydrate-active enzymes in the human gut microbiota. *Nat Rev Microbiol.* 2013;11:497–504.
www.nature.com/reviews/micro
28. Martínez Cruz P, Ibáñez AL, Monroy Hermosillo OA, Ramírez Saad HC. Use of probiotics in aquaculture. *ISRN Microbiol.* 2012;2012:1–13.
<https://www.ncbi.nlm.nih.gov/pmc/articles/PMC3671701/>
29. Torrecillas S, Montero D, Izquierdo M. Improved health and growth of fish fed mannan oligosaccharides: Potential mode of action. *Fish Shellfish Immunol.* 2014;36:525–44.
<https://www.sciencedirect.com/science/article/pii/S1050464813008991>

30. Naas AE, Pope PB. A mechanistic overview of ruminal fibre digestion. PeerJ. 2019; <https://doi.org/10.7287/peerj.preprints.27831v1>
31. Cerezuela R, Fumanal M, Tapia-Paniagua ST, Meseguer J, Moríñigo M ángel, Esteban M ángeles. Changes in intestinal morphology and microbiota caused by dietary administration of inulin and *Bacillus subtilis* in gilthead sea bream (*Sparus aurata* L.) specimens. Fish Shellfish Immunol. 2013;34:1063–70. <https://www.sciencedirect.com/science/article/pii/S1050464813000363?via%3Dihub>
32. Yang P, Hu H, Liu Y, Li Y, Ai Q, Xu W, et al. Dietary stachyose altered the intestinal microbiota profile and improved the intestinal mucosal barrier function of juvenile turbot, *Scophthalmus maximus* L. Aquaculture. 2018;486:98–106. <https://www.sciencedirect.com/science/article/pii/S0044848617315181#:~:text=Stachyose supplementation in diets at,mucosal barrier function of turbot.&text=Dietary 5%25 stachyose increased the,and some potential pathogenic bacteria>.
33. Krautkramer KA, Fan J, Bäckhed F. Gut microbial metabolites as multi-kingdom intermediates. Nat Rev Microbiol. 2021;19:77–94. www.nature.com/nrmicro
34. Ringø E, Sperstad S, Myklebust R, Mayhew TM, Olsen RE. The effect of dietary inulin on aerobic bacteria associated with hindgut of Arctic charr (*Salvelinus alpinus* L.). Aquac Res. 2006;37:891–7. <https://onlinelibrary.wiley.com/doi/full/10.1111/j.1365-2109.2006.01509.x>
35. Miao S, Zhao C, Zhu J, Hu J, Dong X, Sun L. Dietary soybean meal affects intestinal homeostasis by altering the microbiota, morphology and inflammatory cytokine gene expression in northern snakehead. Sci Rep. 2018;8:113. www.nature.com/scientificreports/
36. Zhang Q, Yu H, Xiao X, Hu L, Xin F, Yu X. Inulin-type fructan improves diabetic phenotype and gut microbiota profiles in rats. PeerJ. 2018;2018. <https://www.ncbi.nlm.nih.gov/pmc/articles/PMC5835350/>
37. Dewulf EM, Cani PD, Neyrinck AM, Possemiers S, Holle A Van, Muccioli GG, et al. Inulin-type fructans with prebiotic properties counteract GPR43 overexpression and PPAR γ -related adipogenesis in the white adipose tissue of high-fat diet-fed mice. J Nutr Biochem. 2011;22:712–22. <https://pubmed.ncbi.nlm.nih.gov/21115338/>
38. Wang T, Zhang N, Yu X-B, Qiao F, Chen L-Q, Du Z-Y, et al. Inulin alleviates adverse metabolic syndrome and regulates intestinal microbiota composition in Nile Tilapia (*Oreochromis niloticus*) fed with high-carbohydrate diet. Br J Nutr. 2020;1–29. https://www.cambridge.org/core/product/identifier/S000711452000402X/type/journal_article
39. Adebola OO, Corcoran O, Morgan WA. Prebiotics may alter bile salt hydrolase activity: Possible implications for cholesterol metabolism. PharmaNutrition. 2020;12:100182. shorturl.at/fgxW1
40. Reza A, Abdolmajid H, Abbas M, Abdolmohammad AK. Effect of dietary prebiotic inulin on growth performance, intestinal microflora, body composition and hematological parameters of juvenile beluga, *Huso huso* (Linnaeus, 1758). J World Aquac Soc. 2009;40:771–9. <https://onlinelibrary.wiley.com/doi/full/10.1111/j.1749-7345.2009.00297.x>

41. Burr G, Gatlin DM, Hume M. Effects of the prebiotics GroBiotic® -A and inulin on the intestinal microbiota of red drum, *sciaenops ocellatus*. J World Aquac Soc. 2009;40:440–9. <https://onlinelibrary.wiley.com/doi/full/10.1111/j.1749-7345.2009.00271.x>
42. Burr G, Hume M, Ricke S, Nisbet D, Gatlin D. *In Vitro* and *in vivo* evaluation of the prebiotics GroBiotic®-A, inulin, mannanoligosaccharide, and galactooligosaccharide on the digestive microbiota and performance of hybrid striped bass (*Morone chrysops* × *Morone saxatilis*). Microb Ecol. 2010;59:187–98. <https://pubmed.ncbi.nlm.nih.gov/19844649/>
43. Hill JH, Franzosa EA, Huttenhower C, Guillemin K. A conserved bacterial protein induces pancreatic beta cell expansion during zebrafish development. Elife. 2016;5:18. <https://www.ncbi.nlm.nih.gov/pmc/articles/PMC5154760/>
44. Rolig AS, Parthasarathy R, Burns AR, Bohannan BJM, Guillemin K. Individual members of the microbiota disproportionately modulate host innate immune responses. Cell Host Microbe. 2015;18:613–20. <http://www.ncbi.nlm.nih.gov/pubmed/26567512>
45. Rolig AS, Sweeney EG, Kaye LE, Desantis MD, Perkins A, Banse A V., et al. A bacterial immunomodulatory protein with lipocalin-like domains facilitates host–bacteria mutualism in larval zebrafish. Elife. 2018;7. <https://elifesciences.org/articles/37172>
46. Razin S, Yogev D, Naot Y. Molecular biology and pathogenicity of mycoplasmas. Microbiol Mol Biol Rev. 1998;62:1094–156. <http://mmlbr.asm.org/>
47. Razin S. Molecular biology and genetics of mycoplasmas (Mollicutes). Microbiol Rev. 1985;49:419–55. <https://www.ncbi.nlm.nih.gov/pmc/articles/PMC373046/>
48. Rimoldi S, Gini E, Iannini F, Gasco L, Terova G. The effects of dietary insect meal from *Hermetia illucens* prepupae on autochthonous gut microbiota of rainbow trout (*Oncorhynchus mykiss*). Animals. 2019;9. <https://pubmed.ncbi.nlm.nih.gov/30987067/>
49. Llewellyn MS, McGinnity P, Dionne M, Letourneau J, Thonier F, Carvalho GR, et al. The biogeography of the Atlantic salmon (*Salmo salar*) gut microbiome. ISME J. 2016;10:1280–4. <http://www.ncbi.nlm.nih.gov/pubmed/26517698>
50. Lokesh J, Kiron V, Sipkema D, Fernandes JMO, Moum T. Succession of embryonic and the intestinal bacterial communities of Atlantic salmon (*Salmo salar*) reveals stage-specific microbial signatures. Microbiologyopen. 2019;8. <https://onlinelibrary.wiley.com/doi/full/10.1002/mbo3.672>
51. Rasmussen JA, Villumsen KR, Duchêne DA, Puetz LC, Delmont TO, Sveier H, et al. Genome-resolved metagenomics suggests a mutualistic relationship between *Mycoplasma* and salmonid hosts. Commun Biol. 2021;4:1–10. <https://www.nature.com/articles/s42003-021-02105-1>
52. Cheaib B, Yang P, Kazlauskaitė R, Lindsay E, Heys C, Dwyer T, et al. Genome erosion and evidence for an intracellular niche – exploring the biology of mycoplasmas in Atlantic salmon. Aquaculture. 2021;541:736772. <https://www.sciencedirect.com/science/article/pii/S0044848621004348#f0005>
53. Lian CA, Yan GY, Huang JM, Danchin A, Wang Y, He LS. Genomic characterization of a novel gut symbiont from the hadal snailfish. Front Microbiol. 2020;10:2978. [shorturl.at/ehkoF](https://www.frontiersin.org/shorturl.at/ehkoF)

54. Bozzi D, Rasmussen JA, Carøe C, Sveier H, Nordøy K, Gilbert MTP, et al. Salmon gut microbiota correlates with disease infection status: potential for monitoring health in farmed animals. *Anim Microbiome*. 2021;3. <https://www.ncbi.nlm.nih.gov/pmc/articles/PMC8056536/>
55. Rottem S. Interaction of mycoplasmas with host cells. *Physiol Rev*. 2003;83:417–32. <https://pubmed.ncbi.nlm.nih.gov/12663864/>
56. Waites KB, Talkington DF. *Mycoplasma pneumoniae* and its role as a human pathogen. *Clin Microbiol Rev*. 2004;17:697–728. <http://cmr.asm.org/>
57. Wang A, Zhang Z, Ding Q, Yang Y, Bindelle J, Ran C, et al. Intestinal *Cetobacterium* and acetate modify glucose homeostasis via parasympathetic activation in zebrafish. *Gut Microbes*. 2021;13:1–15. <https://www.tandfonline.com/action/journalInformation?journalCode=kgmi20>
58. Park SS, Yang G, Kim E. *Lactobacillus acidophilus* NS1 reduces phosphoenolpyruvate carboxylase expression by regulating HNF4 α transcriptional activity. *Korean J Food Sci Anim Resour*. 2017;37:529–34. <https://www.ncbi.nlm.nih.gov/pmc/articles/PMC5599573/>
59. Den Besten G, Van Eunen K, Groen AK, Venema K, Reijngoud DJ, Bakker BM. The role of short-chain fatty acids in the interplay between diet, gut microbiota, and host energy metabolism. *J Lipid Res*. 2013;54:2325–40. <https://www.ncbi.nlm.nih.gov/pmc/articles/PMC3735932/>
60. Edwards M, Mohiuddin SS. Biochemistry, Lipolysis [Internet]. StatPearls. StatPearls Publishing; 2020. <http://www.ncbi.nlm.nih.gov/pubmed/32809399>
61. NRC. Nutrient Requirements of Fish. *Nutr. Requir. Fish*. National Academies Press; 1993.
62. Moore S. Amino acid analysis: aqueous dimethyl sulfoxide as solvent for the ninhydrin reaction. *J Biol Chem*. Elsevier; 1968;243:6281–3. <https://www.sciencedirect.com/science/article/pii/S0021925818944881?via%3Dihub>
63. Folch J, Lees M, Sloane Stanley GH. A simple method for the isolation and purification of total lipides from animal tissues. *J Biol Chem*. 1957;226:497–509. <https://pubmed.ncbi.nlm.nih.gov/13428781/>
64. Good CA, Kramer H, Somogyi M. The determination of glycogen. *J Biol Chem*. 1933;100:485–91. <https://www.sciencedirect.com/science/article/pii/S0021925818759668>
65. Illumina. 16S Metagenomic Sequencing Library Preparation [Internet]. https://support.illumina.com/documents/documentation/chemistry_documentation/16s/16s-metagenomic-library-prep-guide-15044223-b.pdf
66. Klindworth A, Priesse E, Schweer T, Peplies J, Quast C, Horn M, et al. Evaluation of general 16S ribosomal RNA gene PCR primers for classical and next-generation sequencing-based diversity studies. *Nucleic Acids Res*. 2013;41:e1. <http://www.pubmedcentral.nih.gov/articlerender.fcgi?artid=3592464&tool=pmcentrez&rendertype=abstract>
67. Edgar RC. UPARSE: Highly accurate OTU sequences from microbial amplicon reads. *Nat Methods*. 2013;10:996–8. <https://www.nature.com/articles/nmeth.2604>
68. Edgar RC, Flyvbjerg H. Error filtering, pair assembly, and error correction for next-generation sequencing reads. *Bioinformatics*. 2015;31:3476–82.

- <http://www.ncbi.nlm.nih.gov/pubmed/26139637>
69. Edgar RC. Tolstoy's paradox [Internet]. <https://www.drive5.com/usearch/manual/tolstoy.html>
 70. Edgar R. SINTAX: A simple non-Bayesian taxonomy classifier for 16S and ITS sequences. *bioRxiv*. 2016;074161. <https://doi.org/10.1101/074161>
 71. McMurdie PJ, Holmes S. phyloseq: An R package for reproducible interactive analysis and graphics of microbiome census data. *PLoS One*. 2013;8:e61217. <https://dx.plos.org/10.1371/journal.pone.0061217>
 72. Spellerberg IF, Fedor PJ. A tribute to Claude-Shannon (1916-2001) and a plea for more rigorous use of species richness, species diversity and the "Shannon-Wiener" Index. *Glob Ecol Biogeogr*. 2003;12:177–9. <https://onlinelibrary.wiley.com/doi/full/10.1046/j.1466-822X.2003.00015.x>
 73. Ghislain M, Costarramone N, Pigot T, Reyrolle M, Lacombe S, Le Behec M. High frequency air monitoring by selected ion flow tube-mass spectrometry (SIFT-MS): Influence of the matrix for simultaneous analysis of VOCs, CO₂, ozone and water. *Microchem J*. 2020;153:104435. <https://www.sciencedirect.com/science/article/pii/S0026265X19328310>
 74. Ghislain M, Costarramone N, Sotiropoulos JM, Pigot T, Van Den Berg R, Lacombe S, et al. Direct analysis of aldehydes and carboxylic acids in the gas phase by negative ionization selected ion flow tube mass spectrometry: Quantification and modelling of ion–molecule reactions. *Rapid Commun Mass Spectrom*. 2019;33:1623–34. <https://pubmed.ncbi.nlm.nih.gov/31216077/>
 75. Vandesompele J, De Preter K, Pattyn F, Poppe B, Van Roy N, De Paepe A, et al. Accurate normalization of real-time quantitative RT-PCR data by geometric averaging of multiple internal control genes. *Genome Biol*. 2002;3:1–12. <http://genomebiology.com/2002/3/7/research/0034>. 1Correspondence: .rankSpeleman.
 76. R Core Team. R: A language and environment for statistical computing [Internet]. Vienna, Austria: R Foundation for Statistical Computing; 2018. <https://www.r-project.org>
 77. Kohl M. SLqPCR: Functions for analysis of real-time quantitative PCR data at SIRS-Lab GmbH version 1.54.0 from Bioconductor [Internet]. <https://rdrr.io/bioc/SLqPCR/>
 78. Anderson MJ. Distance-based tests for homogeneity of multivariate dispersions. *Biometrics*. 2006;62:245–53. <http://doi.wiley.com/10.1111/j.1541-0420.2005.00440.x>
 79. Oksanen J, Blanchet FG, Friendly M, Kindt R, Legendre P, McGlinn D, et al. vegan: Community ecology package [Internet]. 2018. <https://cran.r-project.org/package=vegan>
 80. Anderson MJ. Permutational multivariate analysis of variance (PERMANOVA). *Wiley StatsRef Stat Ref Online*. 2017;1–15. <https://onlinelibrary.wiley.com/doi/full/10.1002/9781118445112.stat07841>
 81. Kandlikar GS, Gold ZJ, Cowen MC, Meyer RS, Freise AC, Kraft NJB, et al. Ranacapa: An R package and shiny web app to explore environmental DNA data with exploratory statistics and interactive visualizations. *F1000Research*. 2018;7. <https://www.ncbi.nlm.nih.gov/pmc/articles/PMC6305237/>
 82. Rohart F, Gautier B, Singh A, Lê Cao K-A. mixOmics: An R package for 'omics feature selection and multiple data integration. *PLOS Comput Biol*. 2017;13:e1005752. <https://dx.plos.org/10.1371/journal.pcbi.1005752>

Tables

Table 1: Formulation of the diets used in the present study.

Ingredient (%)	Control	Prebiotic 1%	Prebiotic 2%
Wheat gluten	15.00	15.00	15.00
Pea protein	12.50	12.50	12.50
Corn gluten	12.00	12.00	12.00
Traced soybean meal	12.00	12.00	12.00
Lupine flour	10.00	10.00	10.00
Faba bean protein concentrate	8.00	8.00	8.00
Whole wheat	6.13	6.13	6.13
Rapeseed oil	8.88	8.88	8.88
Linseed oil	4.00	4.00	4.00
Palm oil	2.00	2.00	2.00
Soy lecithin powder	2.50	2.50	2.50
Vitamin premix	1.50	1.50	1.50
Mineral premix	0.63	0.63	0.63
Dicalcium Phosphate	1.86	1.86	1.86
L-Lysine	0.50	0.50	0.50
L-Méthionine	0.50	0.50	0.50
Prebiotic*	0.00	1.00	2.00
Cellulose	2.00	1.00	0.00

* Either FOS (Fructo-oligosaccharide), Inulin or MOS (Mannan-oligosaccharide)

Table 2: Growth parameters of fish fed with the control and different experimental diets containing prebiotics.

Growth parameters	Control	FOS1	FOS2	Inulin1	Inulin2	MOS1	MOS2	p value
Feed efficiency ¹	0.86 ± 0.07	0.97 ± 0.03	0.94 ± 0.07	0.95 ± 0.02	0.94 ± 0.04	0.91 ± 0.04	0.93 ± 0	0.137
Final body weight (g)	177.99 ± 27.06	171.28 ± 26.01	166.5 ± 18.1	166 ± 21.63	187.95 ± 24.63	139.38 ± 27.29*	170.68 ± 20.91	2.93e⁻⁰⁵
Hepatosomatic index (%) ²	0.98 ± 0.06	0.95 ± 0.12	1.11 ± 0.18	1.04 ± 0.07	0.99 ± 0.1	1.11 ± 0.12	0.99 ± 0.11	0.046
Protein retention efficiency (%) ³	1.78 ± 0.14	1.99 ± 0.04	1.92 ± 0.10	1.91 ± 0.08	1.95 ± 0.04	1.80 ± 0.03	1.86 ± 0.08	0.063
Specific growth rate (%/day) ⁴	2.04 ± 0.11	2.14 ± 0.04	2.09 ± 0.08	2.03 ± 0.06	2.21 ± 0.06	1.97 ± 0.10	2.12 ± 0.03	0.023
Viscerosomatic index (%) ⁵	10.84 ± 0.99	10.21 ± 1.36	11.02 ± 0.95	11.28 ± 1.57	9.85 ± 1.04	10.71 ± 1.22	10.72 ± 0.84	0.173

The data is presented as the mean ± sd, n=3 tanks except for the final body weight (n=12), hepatosomatic index (n=9) and viscerosomatic index (n=9). Means between the groups were compared using a one-way ANOVA. A p value < 0.05 was considered as significant and are presented in bold.

*MOS1 is significantly different from the control group.

¹Feed efficiency=wet weight gain (g)/feed intake (g).

²Hepatosomatic index=100x (liver weight/total body weight)

³Protein retention efficiency=wet weight gain (g)/crude protein intake (g)

⁴Specific growth rate=100x [Ln (final body weight, g)-Ln (initial body weight, g)]/days

⁵Viscerosomatic index=100x (viscera weight, g/total body weight, g)

Table 3: Measurement of the hepatic and plasma parameters in the fish fed with the control and different experimental diets containing prebiotics.

Parameters	Control	FOS1	FOS2	Inulin1	Inulin2	MOS1	MOS2	p value
Hepatic fat (%)	16.31 ± 1.95	16.76 ± 1.96	17.18 ± 0.87	17.98 ± 1.58	15.89 ± 1.62	18 ± 1.77	17.60 ± 3.27	0.149
Hepatic glycogen (mg/g)	70.02 ± 16.91	83.23 ± 18.45	86.10 ± 19.44	69.10 ± 17.77	83.59 ± 11.89	68.58 ± 20.31	75.16 ± 13.07	0.117
Cholesterol (g/L)	0.62 ± 0.07	0.62 ± 0.13	0.68 ± 0.17	0.72 ± 0.14	0.68 ± 0.13	0.72 ± 0.07	0.7 ± 0.14	0.489
Free fatty acids (mmol/L)	0.29 ± 0.07	0.3 ± 0.03	0.33 ± 0.06	0.29 ± 0.08	0.3 ± 0.04	0.34 ± 0.1	0.28 ± 0.08	0.4585
Glucose (g/L)	1.18 ± 0.19	1.16 ± 0.17	1.14 ± 0.12	1.44 ± 0.51	1.38 ± 0.34	1.32 ± 0.33	1.13 ± 0.26	0.5166
Total amino acids (µmol/mL)	4.38 ± 0.43	4.09 ± 0.42	4.3 ± 0.9	4.51 ± 0.41	3.84 ± 0.48	4.76 ± 1.07	4.41 ± 0.63	0.1946
Triglycerides (g/L)	0.92 ± 0.3	0.81 ± 0.37	0.83 ± 0.36	1.12 ± 0.38	1.09 ± 0.22	1.05 ± 0.34	0.7 ± 0.3	0.069

The data is presented as the mean ± sd, n=9. Means between the groups were compared using a one-way ANOVA. A p value < 0.05 was considered as significant.

Figures

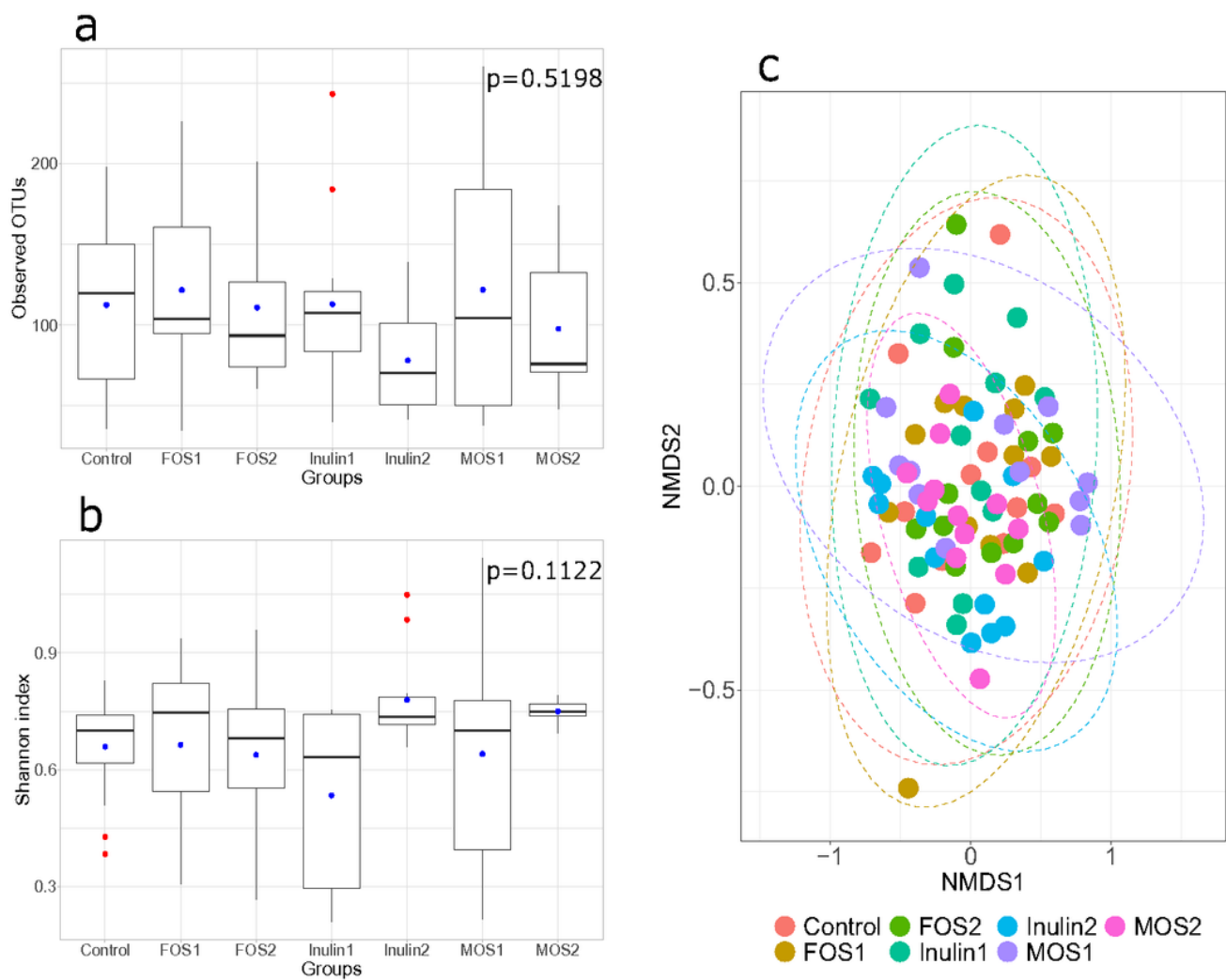


Figure 1

Bacterial alpha diversity represented in terms of observed OTUs (a) and Shannon index (b). Alpha diversity between diet groups was compared using one-way ANOVA and $p < 0.05$ was considered significant. Beta diversity is presented as Bray-Curtis distance between samples and depicted using NMDS (c). Beta diversity was compared using pairwise PERMANOVA and $p < 0.05$ was considered significant, $n=12$.

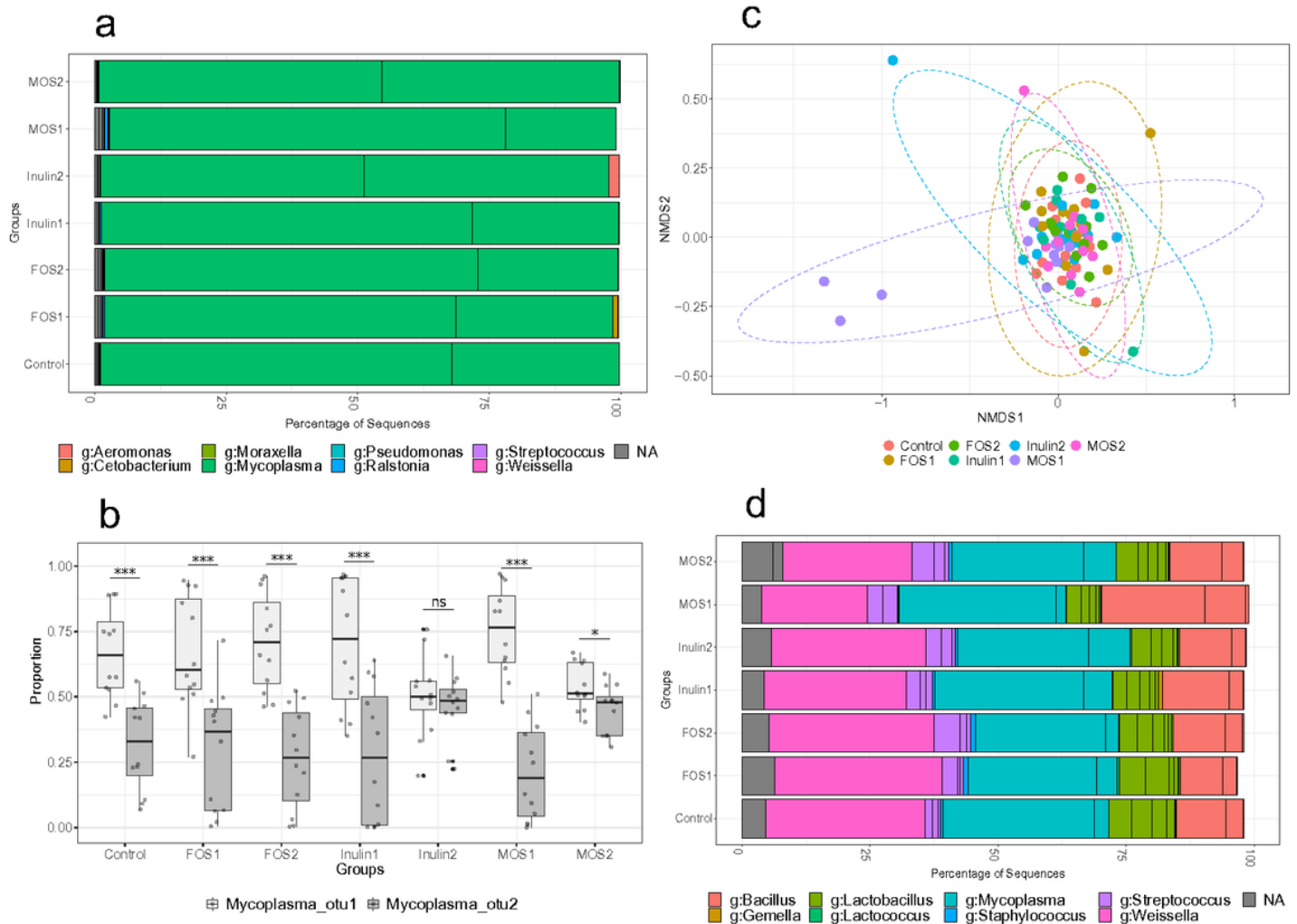


Figure 2

Taxonomic composition of bacterial OTUs using bacterial domain primers (a). Differences in abundance of 2 OTUs belonging to Mycoplasma in different dietary groups (b). Significant differences are indicated with asterisks. NMDS plot showing beta diversity (Bray-Curtis distance) of samples amplified with the Firmicutes-specific primers (c). Beta diversities were compared using pairwise PERMANOVA and $p < 0.05$ was considered significant. Taxonomic composition of bacterial OTUs using the Firmicutes-specific primers (d), $n=12$.

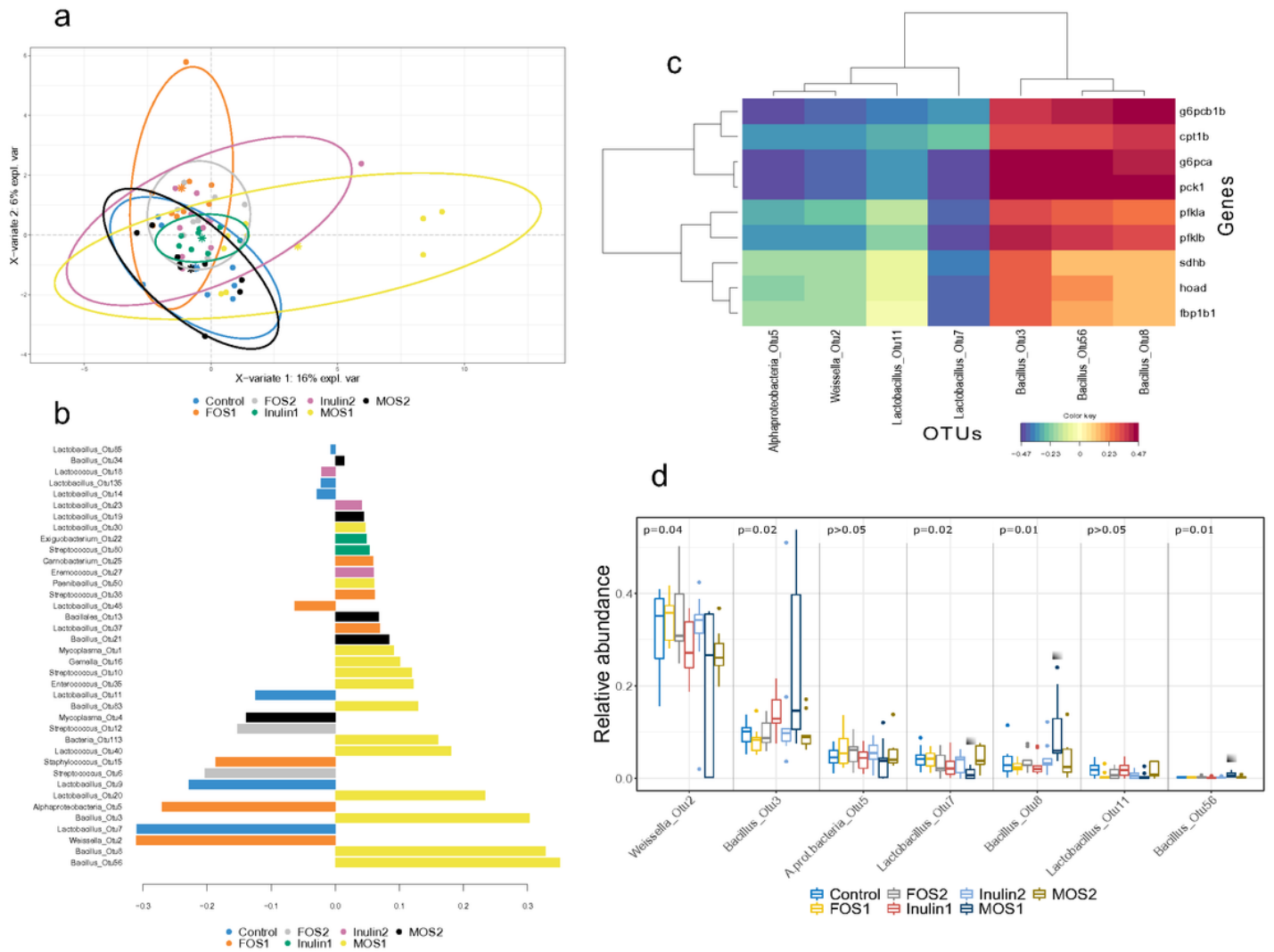


Figure 3

PLS-DA analysis of OTU abundance data generated with the Firmicutes-specific primers (a). Regression coefficients representing the magnitude of variation contributed by each OTU (variable) to the clustering of samples in PLS-DA (b). Heatmap showing the significant correlations calculated using regularised canonical correlation analysis (rCCA) between the OTUs and gene expression levels in liver. A comparison of the relative abundances of OTUs significantly correlated with hepatic gene expression (d). The differences are considered significant at $p < 0.05$. Group-specific differences are highlighted by the square above the boxplot, $n = 9$.

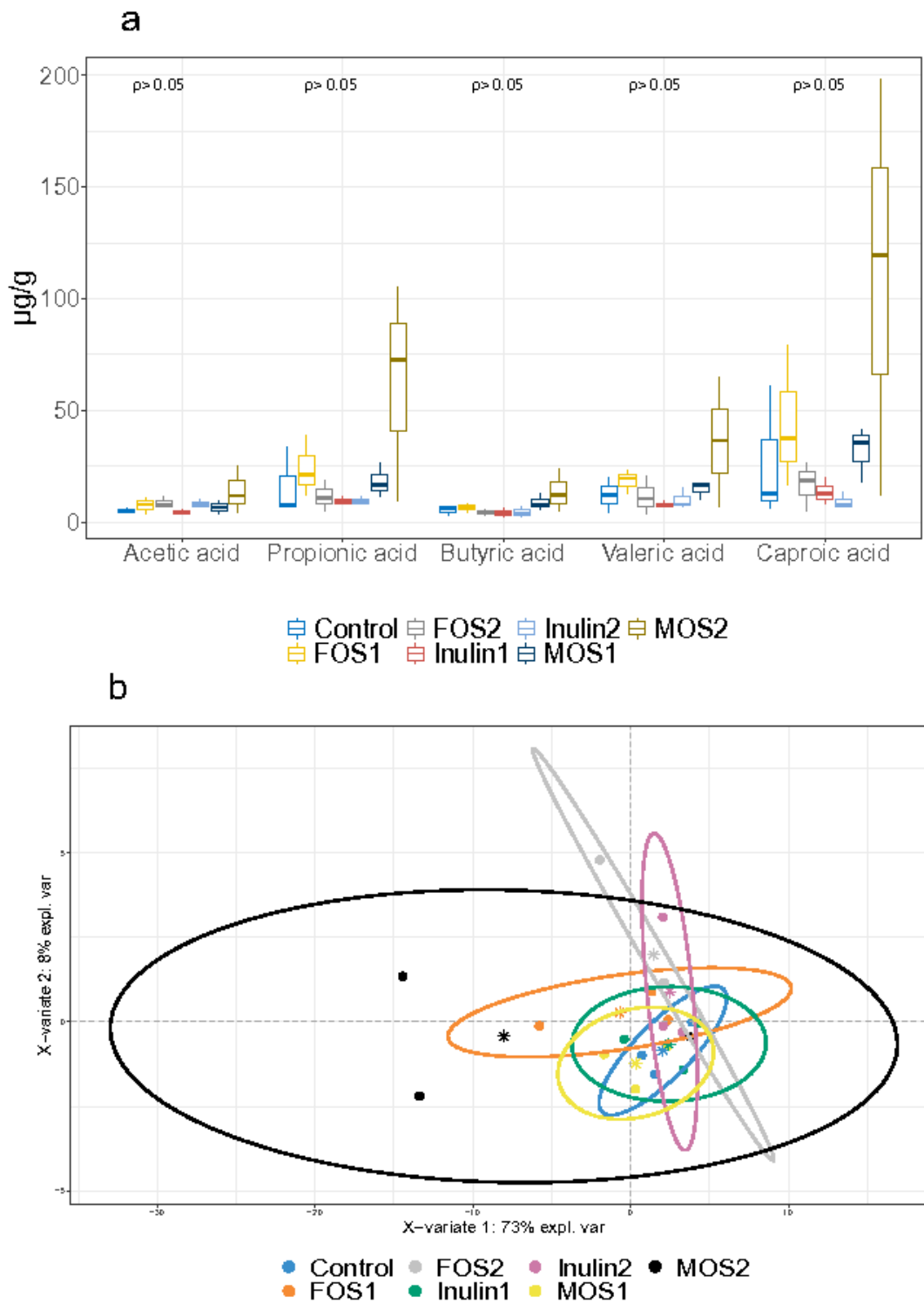


Figure 4

SCFA levels in the intestinal contents of different diet groups (a), and PLS-DA based on the product ions derived from all the SCFAs in intestinal contents (b), n=3.

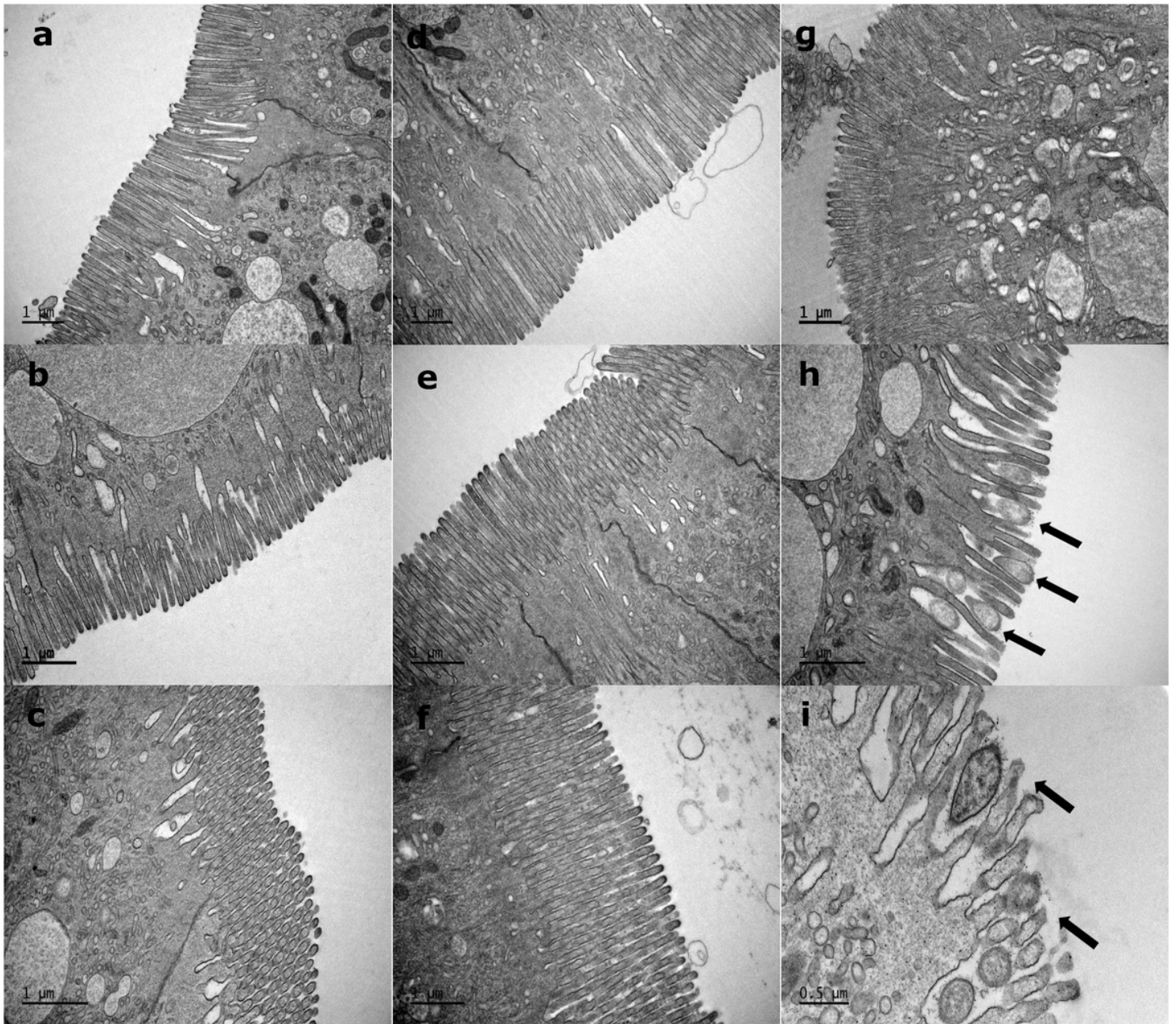


Figure 5

Representative transmission electron micrographs showing the comparison of intestinal microvilli structures between different diet groups, control (a), FOS1(b), FOS2(c), Inulin1(d), Inulin2(e), MOS1(f), MOS2(g). Photomicrograph showing attachment of Mycoplasma to the microvillar structure of intestinal epithelial cells (h). Possible damage to the microvillar structures (indicated by arrow) of intestinal epithelial cells (i).

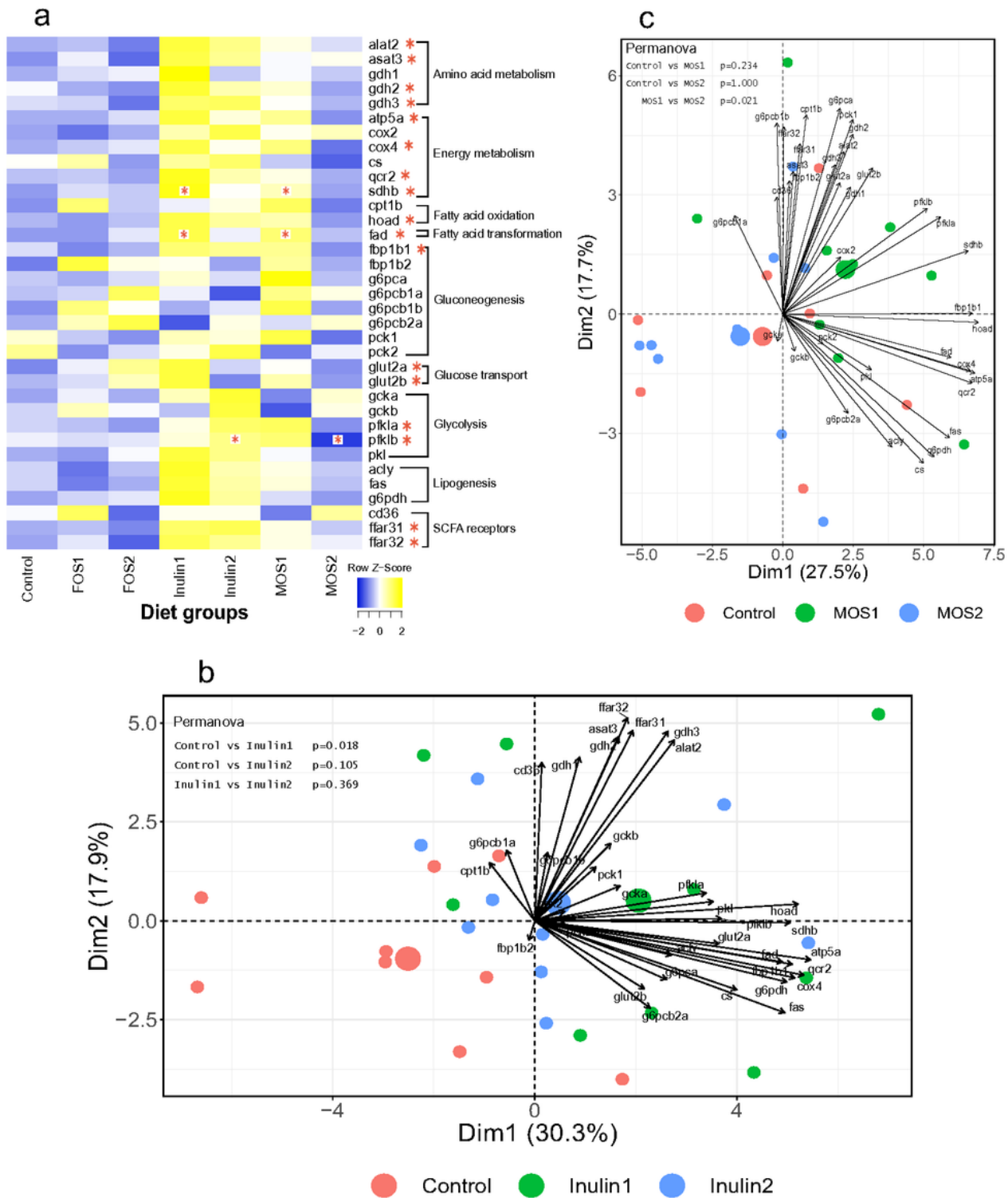


Figure 6

Heatmap showing the expression of genes involved in different metabolic pathways in the liver in response to different dietary prebiotics (a). Principal component analysis shows the differences in overall gene expression between control and inulin (b) and MOS (c) fed groups. The arrows in the plot represent the variables (genes) and the samples are represented by the colour-coded spheres. The mean of the ordination of each group is shown as a larger sphere, $n=9$.

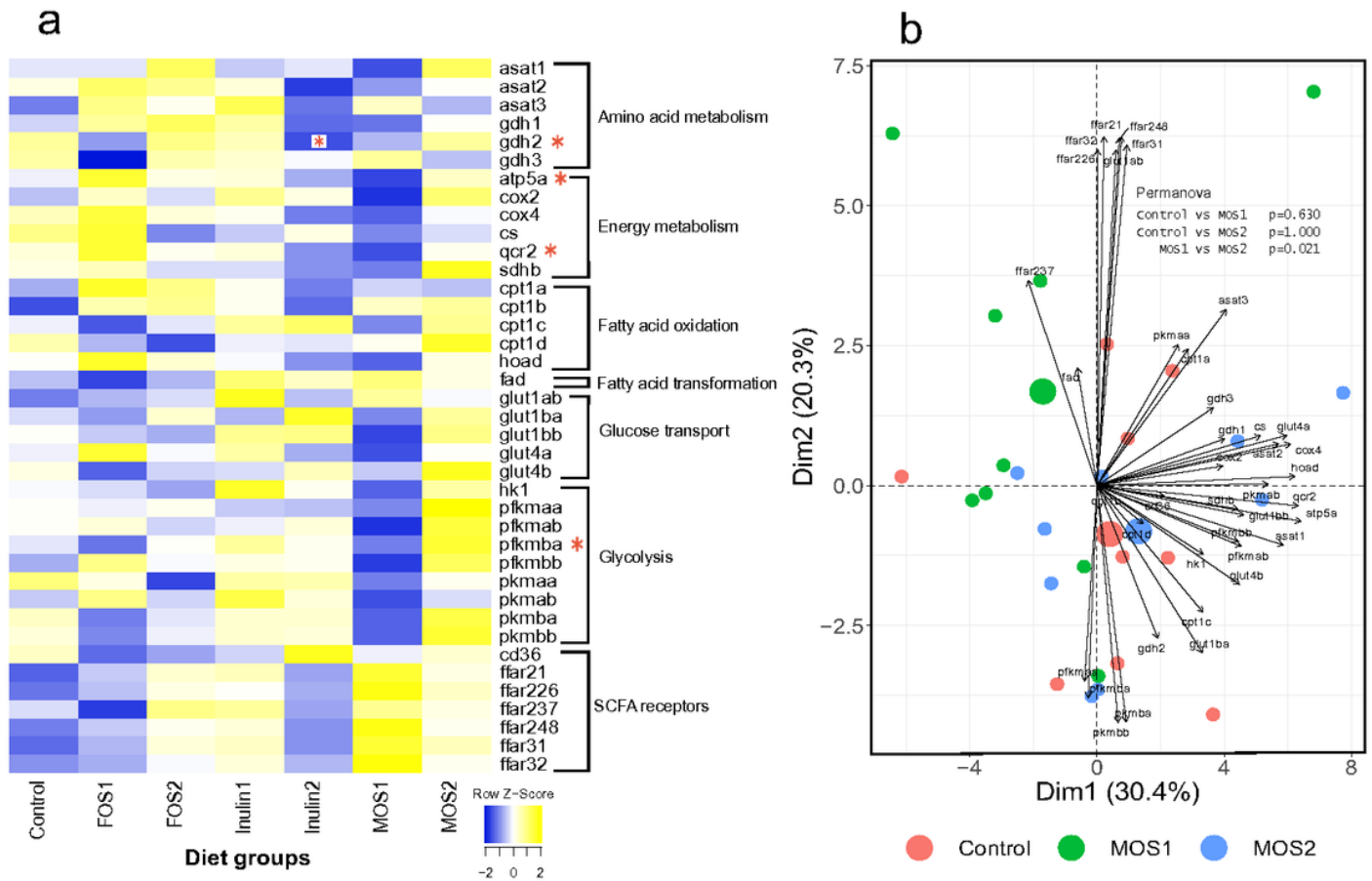


Figure 7

Heatmap showing the expression of genes involved in different metabolic pathways in muscle in response to different dietary prebiotics (a). Principal component analysis showing differences in the overall gene expression between control and MOS fed groups (b). The arrows in the graph represent the variables (genes) and the samples are represented by the colour-coded spheres. The mean of the ordination of each group is shown as a larger sphere, n=9.

Supplementary Files

This is a list of supplementary files associated with this preprint. Click to download.

- [Supplementaryfigure1.pdf](#)
- [Supplementaryfigure2.pdf](#)
- [Supplementaryfigure3.pdf](#)
- [Supplementarytables.docx](#)